JEM Journal of Experimental Medicine

ARTICLE

IEC-intrinsic IL-1R signaling holds dual roles in regulating intestinal homeostasis and inflammation

Garrett R. Overcast[1,3,4*], Hannah E. Meibers[2,3,4*], Emily M. Eshleman[3,4], Irene Saha[3,4], Lisa Waggoner[3,4], Krupaben N. Patel[5], Viral G. Jain[6], David B. Haslam[7,8], Theresa Alenghat[3,4,8], Kelli L. VanDussen[5,8], and Chandrashekhar Pasare[3,4,8]

Intestinal epithelial cells (IECs) constitute a critical first line of defense against microbes. While IECs are known to respond to various microbial signals, the precise upstream cues regulating diverse IEC responses are not clear. Here, we discover a dual role for IEC-intrinsic interleukin-1 receptor (IL-1R) signaling in regulating intestinal homeostasis and inflammation. Absence of IL-1R in epithelial cells abrogates a homeostatic antimicrobial program including production of antimicrobial peptides (AMPs). Mice deficient for IEC-intrinsic IL-1R are unable to clear *Citrobacter rodentium* (*C. rodentium*) but are protected from DSS-induced colitis. Mechanistically, IL-1R signaling enhances IL-22R–induced signal transducer and activator of transcription 3 (STAT3) phosphorylation in IECs leading to elevated production of AMPs. IL-1R signaling in IECs also directly induces expression of chemokines as well as genes involved in the production of reactive oxygen species. Our findings establish a protective role for IEC-intrinsic IL-1R signaling in combating infections but a detrimental role during colitis induced by epithelial damage.

Introduction

The intestine is home to trillions of microbes that co-exist with host immune cells. These immune cells include innate lymphoid cell type 3 (ILC3s), CD103$^+$ dendritic cells, and various subsets of T cells that reside in either the lamina propria (lamina propria lymphocytes: LPLs) or interspersed between the epithelial cells (intraepithelial lymphocytes: IELs; Mowat and Agace, 2014). A monolayer of IECs bound by tight junctions form a dynamic barrier separating the microbial contents of the intestinal lumen from the underlying immune cells in the lamina propria (Kaminsky et al., 2021). Apart from acting as a physical barrier, IECs also play a major role in regulating intestinal immune responses. They are critical for dampening immune responses against commensals (Natividad et al., 2012), but are equally important for initiating immune responses against invasive pathogens (Rauch et al., 2017). A well-defined communication circuit resulting in mucosal tolerance is present between intestinal lymphocytes and IECs. For example, previous studies have found that IELs are positioned to relay signals to IECs and are directly involved in antimicrobial peptide (AMP) production and intestinal homeostasis (Ismail et al., 2011; Das et al., 2003). Additionally, LPLs communicate with IECs through the production of cytokines which involved tissue repair (Pickert et al., 2009). Finally, metabolites produced by the microbiota are known to regulate IEC function. Lactate, acetate, and butyrate have all been shown to contribute to barrier function and regulating microbial communities in the intestinal lumen (Wrzosek et al., 2013; Byndloss et al., 2017; Okada et al., 2013; Rodríguez-Colman et al., 2017). The above examples highlight the communication between IECs, microbes, and lymphocytes in the gut to create a fine balance and maintain homeostasis. Despite this tolerogenic environment, IECs are also particularly sensitive to microbial invasion and respond by secreting cytokines and chemokines that can recruit inflammatory immune cells, pointing to existence of pathogen detection mechanisms (Silberger et al., 2017).

An important question in IEC biology is whether these cells can directly sense microbes or respond only to other cues that result from microbial invasion. A large body of evidence supports important functions for cytosolic pattern recognition receptors in IECs such as NOD1, NOD2, and inflammasome sensors

[1]Immunology Graduate Program, University of Texas Southwestern Medical Center at Dallas, Dallas, TX, USA; [2]Immunology Graduate Program, Cincinnati Children's Hospital Medical Center, University of Cincinnati, Cincinnati, OH, USA; [3]Division of Immunobiology, Cincinnati Children's Hospital Medical Center, Cincinnati, OH, USA; [4]Center for Inflammation and Tolerance, Cincinnati Children's Hospital Medical Center, Cincinnati, OH, USA; [5]Divisions of Gastroenterology, Hepatology, and Nutrition and of Developmental Biology, Cincinnati Children's Hospital Medical Center, Cincinnati, OH, USA; [6]Division of Neonatology, University of Alabama at Birmingham, Birmingham, AL, USA; [7]Division of Infectious Diseases, Cincinnati Children's Hospital Medical Center, Cincinnati, OH, USA; [8]Department of Pediatrics, College of Medicine, University of Cincinnati, Cincinnati, OH, USA.

*G. Overcast and H.E. Meibers contributed equally to this paper. Correspondence to Chandrashekhar Pasare: chandrashekhar.pasare@cchmc.org.

such as NLRC4 in intestinal homeostasis (Kobayashi et al., 2005; Lei-Leston et al., 2017; Chen et al., 2008). While these proteins are particularly adept at sensing microbes that invade the cytoplasmic space, whether IECs can directly sense extracellular pathogens remains more poorly understood. Previous studies have found that IEC-intrinsic expression of the adapter molecule MyD88 serves as an important part of IEC–microbiota crosstalk by dictating the IEC defense program (Gibson et al., 2008; Rakoff-Nahoum et al., 2004; Frantz et al., 2012). MyD88 deficient mice were further found to have intestinal dysbiosis because of impaired IEC responses (Rakoff-Nahoum et al., 2004). Since MyD88 is an adapter molecule used by TLRs as well as IL-1R family members (Deguine and Barton, 2014), the specific contributions of TLR versus IL-1R signaling in IECs during host defense or homeostatic processes remain unexplored. Recent work has found minimal to no expression of TLRs in the small and large intestinal epithelium (Price et al., 2018), as well as weak responsiveness to TLR ligands from IEC cell lines and intestinal organoids (Price et al., 2018; Burgueño and Abreu, 2020). An exception to these observations is TLR5 that recognizes flagellin, which is found to be expressed on the basolateral side of small intestinal crypts (Price et al., 2018; Wahida et al., 2021). TLR4 responses have been found to occur through myeloid cells in the environment surrounding IECs and not on IECs themselves (Hausmann et al., 2021).

Recent studies have also highlighted the importance of communication between IECs and various immune cells residing in the lamina propria, which largely depends on cytokine production (Clark and Coopersmith, 2007). For example, the cytokine IL-22 is primarily produced by lymphocytes, such as T helper (Th) 17/22 cells and ILC3s and signals through IL-22R expressed on IECs to induce AMP secretion (Liang et al., 2006; Pickert et al., 2009), thus contributing to intestinal homeostasis. IL-22 is also critical for preserving gut epithelial integrity by promoting wound healing and tissue repair (Pickert et al., 2009). IL-22 production by lymphocytes is licensed by proximal signals from myeloid cells in the form of cytokines such as IL-1 and IL-23 (Gaffen et al., 2014; Peterson and Artis, 2014). Production of IL-1 and IL-23 is induced by activation of a proinflammatory signaling cascade in response to microbial insult (Jain et al., 2018). Thus, myeloid detection of microbes leads to IL-1R signaling and IL-22 production in LPLs and subsequent induction of AMPs by IECs, thereby maintaining homeostasis at the intestinal mucosa. While the IL-1 family of cytokines has been found to play various critical roles in intestinal homeostasis and inflammation by acting on cells proximal to IECs in the signaling relay network, it is unclear whether IECs have evolved to detect IL-1 directly (Golebski et al., 2019; Moon et al., 2014; Jung et al., 2015; Jain et al., 2018), even though IL-1R expression on IECs has been reported (McGee et al., 1996; Sutherland et al., 1994). While a recent report found a role for IL-1R in intestinal stem cell self-renewal by inducing mesenchymal cells to produce R-spondin 3 (Cox et al., 2021) and a role for IL-1R on IECs in tumorigenesis (Dmitrieva-Posocco et al., 2019), a functional role for IL-1R mediated MyD88-dependent signaling in intestinal immune responses has not been explored.

In this study, we found that IL-1R has a critical role in the functioning of both small and large intestinal epithelial cells. Specific deletion of IL-1R in IECs abrogated the ability of small intestinal epithelial cells to produce a wide range of AMPs. Furthermore, we found that IL-1R alone was not sufficient to drive the antimicrobial gene program, but instead acted in synergy with IL-22R signaling to drive an optimal AMP response. We also found that mice with IEC-intrinsic deletion of IL-1R were defective in clearing *Citrobacter rodentium* infection leading to persistent inflammation. Paradoxically, absence of IL-1R in IECs protected mice from dextran sulfate sodium (DSS)–induced colitis, suggesting a pathological role for IL-1R signaling during acute tissue inflammation. We found that IL-1R–dependent induction of chemokines and ROS production led to enhanced recruitment of proinflammatory immune cells and contributed to the tissue damage observed. Together, this study establishes a dual role for IEC-intrinsic IL-1R signaling in maintaining intestinal homeostasis by combating intestinal microbial pathogens as well as acting as a major driver of damage and pathology following disruption of the intestinal barrier.

Results

Epithelial cell–intrinsic IL-1R signaling dictates intestinal antimicrobial program

Previous studies have demonstrated that IEC antimicrobial gene expression is dependent on the signaling adaptor MyD88 (Rakoff-Nahoum et al., 2004). Since the specific contributions of TLR versus IL-1R signaling in IECs remain unexplored and IL-1R signaling pathway utilizes MyD88, we sought to investigate the expression of *Il1r1*, the gene encoding for IL-1R, in IECs and test whether IL-1R signaling is critical to maintain the intestinal antimicrobial gene program. An IL-1R global restore reporter (*Il1r1*$^{GR/GR}$) mouse has been previously developed and reported (Song et al., 2018a). *Il1r1*$^{GR/GR}$ mice co-expresses TdTomato in any cell that expresses IL-1R protein. We enriched for IECs and used flow cytometry to assess IEC TdTomato expression. We detected a small population of IECs in the small intestine and a larger proportion of IECs in the large intestine that were TdTomato$^+$ (Fig. S1 A). Accordingly, immunofluorescent microscopy of *Il1r1*$^{GR/GR}$ colonic tissue showed broad expression of TdTomato that overlapped with E-Cadherin, indicating IEC-specific IL-1R expression (Fig. 1 A and Fig. S1 B). IL-1R was also expressed in the cells of the lamina propria (Fig. 1 A). In the small intestine, overt TdTomato expression was not observed in E-cadherin–positive epithelial cells, possibly reflecting low expression of IL-1R by these cells (Fig. 1 A and Fig. S1 B). There was apparent expression of *Il1r1* transcript in isolated mRNA from both the small intestine and colon epithelial cells (Fig. S1 C). We next wanted to understand the functionality of IL-1R on both small and large intestinal IECs. Analysis of the intestinal epithelium from *Il1r1*$^{-/-}$ (IL-1R KO) mice revealed that gene expression of key antimicrobial peptides, *Reg3g* and *Reg3b* as well as other antimicrobial genes, were significantly abrogated in the absence of IL-1R signaling (Fig. 1 B).

IL-1R signaling plays a critical role in multiple cell types of both the innate and adaptive immune systems. Specifically,

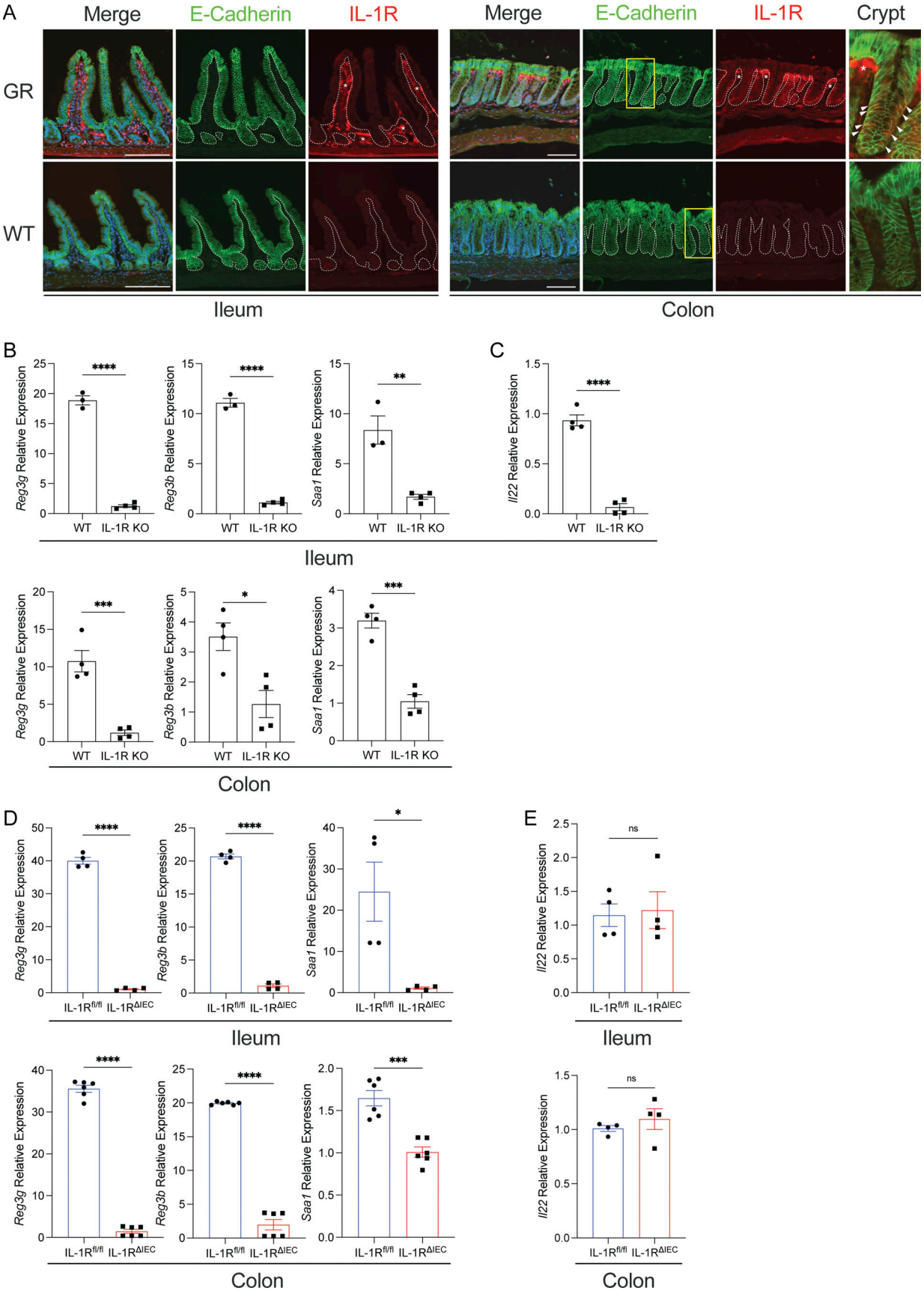

Figure 1. **Epithelial cell–intrinsic IL-1R signaling dictates intestinal antimicrobial program. (A)** IECs constitutively express IL-1R. Histological sections of the large intestine of WT or *Il1r1*$^{GR/GR}$ mice (GR) which co-express TdTomato (red) with IL-1R were co-stained with AF488-E-Cadherin (green) and

counterstained with Hoechst (blue). Asterisks indicate IL-1R expression within the lamina propria. Scale = 100 µm. **(B)** Expression of key antimicrobial effectors is IL-1R dependent. Gene expression was quantitated by real-time qPCR in ileum and colon of WT and *Il1r1*$^{-/-}$ (IL-1R KO) mice (n = 3–4 mice per group). **(C)** IL-1R KO mice have impaired *Il22* expression. *Il22* transcripts were measured in the ileum of WT and IL-1R KO mice by qPCR. **(D)** Expression of key antimicrobial effectors is dependent on IEC-specific IL-1R. Gene expression was quantitated by qPCR of cDNA obtained from ileum and colon of IL-1R$^{fl/fl}$ and IL-1R$^{\Delta IEC}$ mice (n = 4–6 mice per group). **(E)** IL-1R$^{\Delta IEC}$ mice have normal *Il22* expression. *Il22* transcripts were measured in the ileum and colon of IL-1R$^{fl/fl}$ and IL-1R$^{\Delta IEC}$ mice by qPCR (n = 4 mice per group). All mice used in B and C were co-housed for at least 3 wk. All mice used in D and E were littermates. All qPCR assays were run in duplicate and are shown as mean values normalized to *Hprt1*. Data represent at least three independent experiments. Error bars indicate ± SEM. *P < 0.05, **P < 0.01, ***P < 0.001, and ****P < 0.0001. **(B–E)** Unpaired t test.

IL-1R signaling in CD4 T cells (Jain et al., 2018) and ILC3s (Coccia et al., 2012) has been shown to regulate the production of IL-22. Thus, it is possible that impaired expression of AMPs and other genes in IL-1R KO mice could be a result of reduced IL-22 production. We examined *Il22* mRNA transcripts in the intestines of WT and IL-1R KO mice and indeed found a significant defect in its expression in IL-1R KO mice compared to WT mice (Fig. 1 C; Cox et al., 2021; Sutton et al., 2009; Doisne et al., 2011; Chen et al., 2013). While the defect in AMPs could be a result of reduced IL-22 production in IL-1R KO mice, we wanted to examine whether absence of IL-1R specifically on IECs affected their AMP production. We generated *Il1r1*$^{fl/fl}$ × Villin Cre-Tg; (IL-1R$^{\Delta IEC}$; Robson et al., 2016) mice and confirmed IEC-specific deletion by enriching for IECs from small and large intestine as well as splenocytes and measuring expression of *Il1r1* (Fig. S1, D and E). IL-1R$^{\Delta IEC}$ mice have comparable, if not increased, expression of IL-1R on LPLs compared to littermate controls, indicating an IEC-specific deletion of IL-1R (Fig. S1 F). When we tested the AMP expression in small and large intestinal tissues, we found their expression to be significantly compromised in the intestinal epithelium of IL-1R$^{\Delta IEC}$ mice (Fig. 1 D). Importantly, there was no difference in *Il22* or *Epcam* expression in IL-1R$^{\Delta IEC}$ mice in the ileum or colon (Fig. 1 E and Fig. S1 G) suggesting that the defect in the antimicrobial gene program was not due to reduced IL-22 production. While we have not specifically examined the expression of IL-1R on Th17 lineage cells and ILC3s that are known to produce IL-22 in response to IL-1, these results strongly suggest that IEC-intrinsic IL-1R signaling is critical for induction of a broad antimicrobial gene program.

Mucosal immune responses against *C. rodentium* and clearance are dependent on IL-1R signaling in IECs

We next wanted to test the physiological relevance of the impaired antimicrobial program in IL-1R$^{\Delta IEC}$ mice. *C. rodentium* is an attaching and effacing Gram-negative bacterial pathogen that is used to model human infections with *Escherichia coli* and enterohaemorrhagic *E. coli* (Collins et al., 2014). *C. rodentium* predominantly infects the colon of mice and is cleared through the production of AMPs, antibodies, and by the recruitment of immune cells such as neutrophils (Mullineaux-Sanders et al., 2019). We therefore set out to test the role of IEC-intrinsic IL-1R signaling in mediating protection from *C. rodentium* infection. A previous report indicated that differences in microbiome composition in mice can lead to altered intestinal damage and inflammation caused by *C. rodentium* (Lebeis et al., 2009), and that microbiome composition can influence AMP expression in the mouse intestine (Cheng et al., 2019). Therefore, we first examined microbiota composition in IL-1R$^{fl/fl}$ and IL-1R$^{\Delta IEC}$ mice and surprisingly found no major differences in the bacterial taxa suggesting that steady-state composition of commensal microbiota was not affected by the absence of IL-1R signaling in IECs (Fig. S2 A). IL-1R$^{\Delta IEC}$ and IL-1R$^{fl/fl}$ littermate mice were then infected by oral gavage with 2 × 10^9 CFU/mouse *C. rodentium* and monitored for bacterial burden over time (Fig. 2 A). We found no difference in establishment of colonization by the bacteria (first 10 d). However, after 2 wk, the IL-1R$^{fl/fl}$ mice began to clear the infection while the IL-1R$^{\Delta IEC}$ mice continued to shed the pathogen (Fig. 2, A and B). At day 37 after infection, when IL-1R$^{fl/fl}$ mice had completely cleared the infection but IL-1R$^{\Delta IEC}$ still carried bacterial burden, we sacrificed the mice to examine tissue pathology as well as antimicrobial gene expression. Previous reports have indicated that peak IL-22 production and subsequent increases in AMPs occur during early stages of *C. rodentium* infection in mice (Zheng et al., 2008). Consistent with this, we found no difference in AMP expression between WT and IL-1R$^{\Delta IEC}$ mice at the peak of infection (day 11); however, expression of both *Reg3g* and *Lcn2* were impaired in IL-1R$^{\Delta IEC}$ mice at day 37 (Fig. 2 C), which might contribute to lack of clearance of the pathogen. Additionally, we found that IL-1R$^{\Delta IEC}$ mice had shorter colons compared to IL-1R sufficient controls, thus displaying a sign of *C. rodentium*–induced colitis (Fig. 2 D). Histological examination of the colon revealed presence of patches containing inflammatory cell infiltrates in IL-1R$^{\Delta IEC}$ infected mice which were significantly reduced in the IL-1R$^{fl/fl}$ controls (Fig. 2 E and Fig. S2 B).

To ensure that delayed *C. rodentium* clearance is not due to defective generation of adaptive immune responses, we examined the status of *C. rodentium*–specific Th17 responses in both groups of mice. Mesenteric lymph nodes were harvested 11 d after *C. rodentium* infection in IL-1R$^{\Delta IEC}$ and IL-1R$^{fl/fl}$ littermate mice and restimulated with *C. rodentium* lysates for 3 d. We observed no difference in the quantities of secreted IL-17A or IL-22 between T cells derived from IL-1R$^{\Delta IEC}$ and IL-1R$^{fl/fl}$ control mice (Fig. 2 F and Fig. S2 C). In parallel, *C. rodentium*–specific IgG antibodies could also be playing a role in later stages of pathogen clearance, as discussed in a previous report (Kamada et al., 2015). Overall, these data indicate that IEC-intrinsic IL-1R does not dictate development of Th17 responses but plays a direct and important role in clearing *C. rodentium* infection. Since there were no differences in either early AMP production or generation of IL-17 and IL-22 producing CD4 T cells, further studies, including examination of antibodies against *C. rodentium*, are needed to reach definitive conclusions on how absence of IL-1R signaling in IECs regulates the late-stage susceptibility to *C. rodentium* infection.

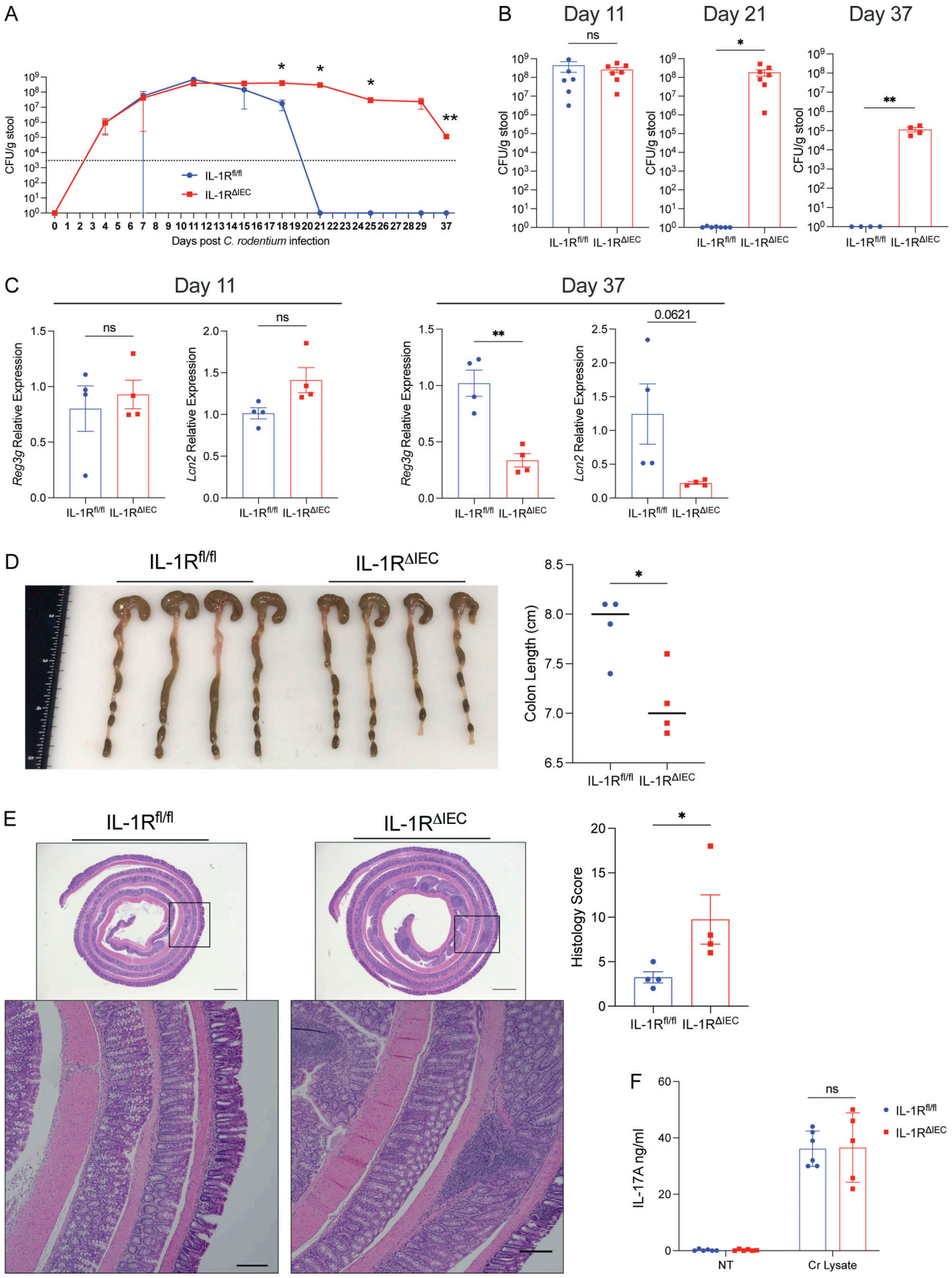

Figure 2. **Mucosal immune responses against *C. rodentium* and clearance are dependent on IL-1R signaling in IECs.** IL-1R$^{fl/fl}$ and IL-1R$^{\Delta IEC}$ mice were orally infected with *C. rodentium* at a dose of 2 × 10^9 CFU/mouse (n = 4–7 mice per group). **(A)** *C. rodentium* load measured in stools of mice on indicated days

after infection. **(B)** *C. rodentium* load in stools of individual mice on days 11, 21, and 37 after infection. **(C)** Gene expression was quantitated by qPCR in large intestines of IL-1R$^{fl/fl}$ and IL-1R$^{\Delta IEC}$ mice at days 11 and 37 after infection. **(D)** Colon lengths of IL-1R$^{fl/fl}$ and IL-1R$^{\Delta IEC}$ mice at day 37 after *C. rodentium* infection. **(E)** Representative H&E-stained colon sections at day 37 following *C. rodentium* infection. Scale = 1,000 µm (top) and 200 µm (bottom). **(F)** IL-17A ELISA on supernatants of mesenteric lymph node cells from *C. rodentium*–infected mice cultured in the presence of *C. rodentium* lysate for 3 d. All mice used were littermates housed together. Data represent two independent experiments (n = 3–7 mice per group). Error bars indicate ± SEM. *P < 0.05 and **P < 0.01. **(A)** Multiple unpaired *t* test. **(B–F)** Unpaired *t* test.

IL-1β synergizes with IL-22 to drive an antimicrobial program by enhancing phosphorylation of STAT3

To understand the mechanisms underlying the role of IEC-intrinsic IL-1R signaling in inducing an antimicrobial gene program, we took advantage of mouse organoid cultures and examined their responses to IL-1β stimulation. *Il1r1*$^{GR/GR}$ mice were used to develop colon epithelial–derived colonoids and imaged to determine IL-1R expression. TdTomato signal was observed in colonoids derived from *Il1r1*$^{GR/GR}$ mice but absent in non-reporter controls, indicating steady-state IL-1R expression in colonic IECs (Fig. S3 A). Organoids derived from the large intestine (colonoids) and small intestine (enteroids) were both found to express *Il1r1* gene transcripts at steady state with colonoids expressing markedly more mRNA for *Il1r1* when compared to enteroids (Fig. S3 B), reflecting the in vivo expression data. In enteroids and colonoids, stimulation with IL-22, a known inducer of AMPs, led to robust transcriptional induction of *Reg3g*, whereas stimulation with IL-1β did not (Fig. 3 A and Fig. S3 C; Keir et al., 2020). Interestingly, when enteroids and colonoids were stimulated simultaneously with IL-22 and IL-1β, there was a robust induction of *Reg3g* that was significantly higher than the induction seen by IL-22 alone (Fig. 3 A and Fig. S3 C). These data suggest that IL-1β by itself cannot induce *Reg3g* expression, but rather synergizes with IL-22 to enhance AMP gene expression. Consistent with the IL-1R expression data, the synergy between IL-22R and IL-1R signaling was more robust in colonoids than enteroids (Fig. 3 A and Fig. S3 C). To test whether the synergy between IL-1β and IL-22 in mouse intestinal tissues was also conserved in human intestinal epithelium, we used biopsy tissue–derived human rectal spheroids from six independent donors (VanDussen et al., 2015). The rectal spheroids were stimulated with IL-1β, IL-22, or both for 12 h. Simultaneous sensing of IL-1β and IL-22 by human rectal epithelial cells led to higher expression of *REG3A* (the human ortholog of *Reg3g*), *LCN2*, and *S100A9* compared to IL-22 alone (Fig. 3 B). These data indicate that the synergy between the IL-1β and IL-22 cytokine receptors that regulates gene transcription is conserved between mouse and human IECs.

The IL-22–mediated AMP program is critically dependent on activation of STAT3 (Pickert et al., 2009). Indeed, IL-22 stimulation of colonoids led to robust phosphorylation of tyrosine 705 of STAT3 (pSTAT3) within 15 min, whereas IL-1β stimulation alone did not induce any pSTAT3 consistent with its failure to induce AMPs (Fig. 3 C). We examined the kinetics of pSTAT3 in colonoids when they were stimulated with both IL-1β and IL-22. Combination treatment of colonoids with IL-22 and IL-1β led to enhanced pSTAT3 when compared to IL-22 alone with the most appreciable increase at 15 min (Fig. 3 D). To investigate the synergy between IL-22R and IL-1R signaling in vivo, WT C57BL/6 mice were injected intraperitoneally with IL-1β, IL-22, or both, and the phosphorylation status of STAT3 was assessed in the colon at 30 min. In agreement with our findings in vitro, we found that IL-1β alone did not trigger STAT3 phosphorylation; however, when combined with IL-22 there was enhanced phosphorylation of STAT3 compared to IL-22 alone (Fig. 3 E). More interestingly, we found enhanced STAT3 phosphorylation only occurred in IL-1R$^{fl/fl}$ and not in IL-1R$^{\Delta IEC}$ mice, indicating this enhanced phosphorylation was dependent on IEC-intrinsic IL-1R signaling (Fig. 3 E). In further agreement with our in vitro findings, combined injection of IL-1β and IL-22 led to rapid upregulation (1 h following injection) of *Reg3g* and *Nos2* expression in colons of mice (Fig. 3 F). These data provide strong in vivo evidence for synergy between IL-22R and IL-1R that leads to enhancement of STAT3 phosphorylation and induction of an antimicrobial gene program. Perplexingly, we found that injection of IL-1β and IL-22 into IL-1R$^{\Delta IEC}$ mice resulted in reduced pSTAT3 in the colonic tissue when compared to IL-22 alone (Fig. 3 G), suggesting that injected IL-22 depends on endogenous IL-1 in vivo or intact epithelial cell intrinsic IL-1R signaling to induce optimal STAT3 phosphorylation in IECs. In agreement with these in vivo data, we discovered that in vitro stimulation of IL-1R$^{\Delta IEC}$–derived colonoids led to defective AMP gene expression when compared to WT colonoids (Fig. 3 H). Additionally, the synergy between IL-1β and IL-22 was lost in IL-1R$^{\Delta IEC}$–derived colonoids (Fig. 3 H). The IL-1R dependence of IL-22 to drive AMP production becomes evident when IL-1R expression is absent in IECs both in vivo and in vitro and needs further examination.

IL-1β and IL-22 drive distinct IEC transcriptional programs

To better understand the outcome of synergy between IL-1R and IL-22R signaling in IECs, we performed mRNA sequencing on mouse intestinal colonoids stimulated with IL-22, IL-1β, or a combination of both for 12 h (Fig. 4). Principal component analysis revealed four individual groups of genes that coincided with each stimulation condition (Fig. 4 A). We found numerous differentially expressed genes that were synergistically induced by combination treatment compared to IL-22 alone, including *Reg3g* and other antimicrobial genes (Fig. 4 B). There were three independent clusters of differentially expressed genes ($Log_2FC > 1.0$) in each of our stimulations totaling 408 genes (Fig. 4 C). Cluster I represents genes that are only induced when there is combined stimulation with IL-1β and IL-22. The genes in cluster I include genes involved in metal ion binding and protease binding (Fig. 4 D). Cluster II represents genes that are synergistically induced by a combination of IL-1β and IL-22 resulting in higher expression than IL-22 alone. These genes are involved in antimicrobial defense, chemokine activity, and protein tyrosine kinase activity (Fig. 4, B and D). Cluster III includes genes that

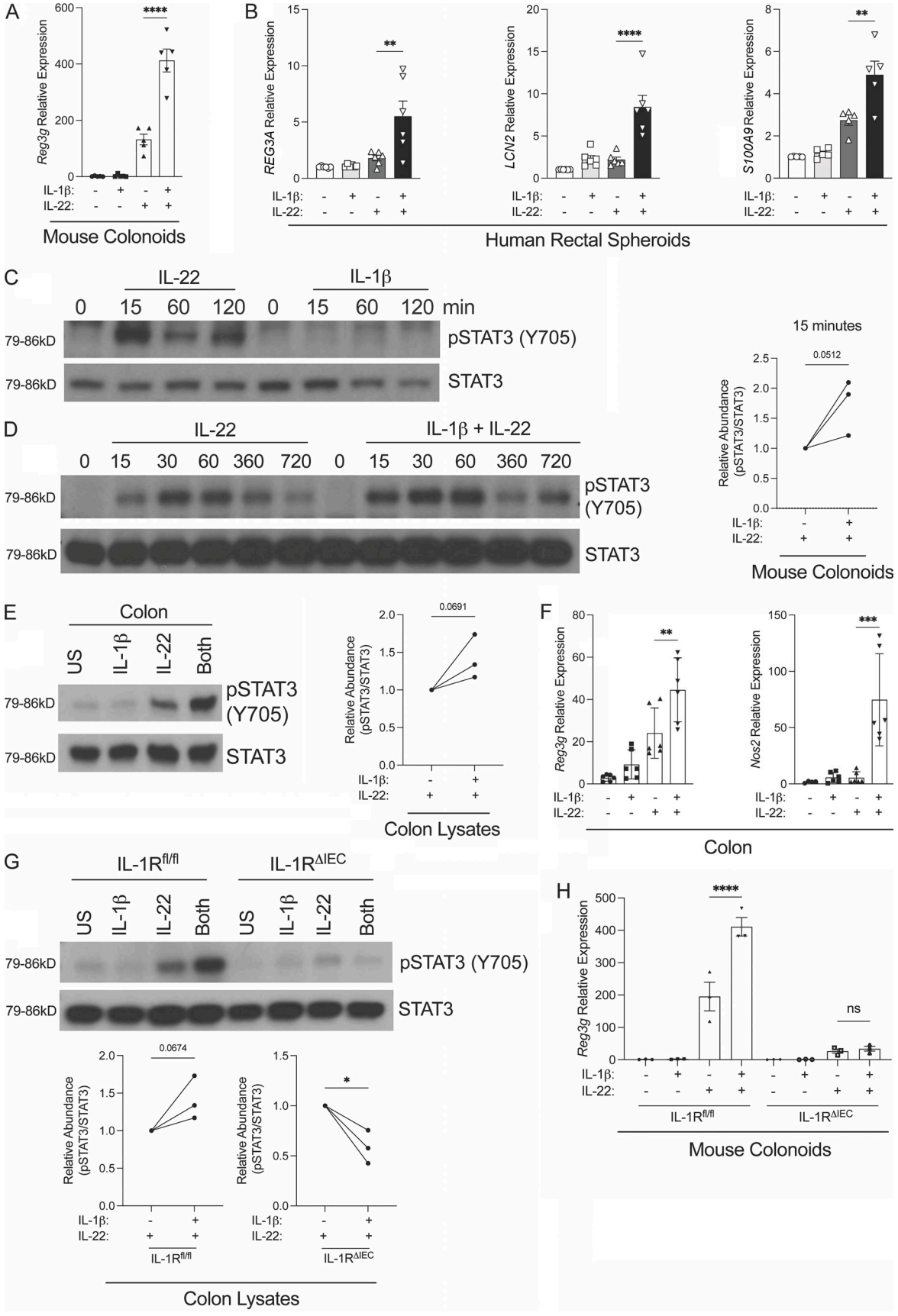

Figure 3. **IL-1β synergizes with IL-22 to drive an antimicrobial gene program by enhancing phosphorylation of STAT3. (A)** IL-1β synergizes with IL-22 for *Reg3g* expression in mouse organoids. Gene expression was quantitated by qPCR of *Reg3g* in colonoids derived from WT mice after a 12-h stimulation

by IL-1β (100 ng/ml), IL-22 (1 ng/ml), or a combination of both. Data represent five independent experiments (n = 5 mice per group). **(B)** IL-22R and IL-1R signaling synergize in human rectal spheroids to influence antimicrobial gene expression. Indicated gene transcripts were quantitated by qPCR in rectal derived spheroids from six independent healthy human donors stimulated for 12 h using IL-1β (100 ng/ml), IL-22 (1 ng/ml), or a combination of both. Data represent two independent experiments. **(C)** Western blot analysis of pSTAT3 and total STAT3 protein of whole cell lysates from colonoids stimulated with IL-22 (1 ng/ml) or IL-1β (100 ng/ml) for indicated periods of time. **(D)** Left: IL-1β synergizes with IL-22 to enhance phosphorylation of STAT3. Western blot analysis of pSTAT3 and total STAT3 protein from whole cell lysates of colonoids stimulated by IL-22 (1 ng/ml) or IL-22 (1 ng/ml) + IL-1β (100 ng/ml) for indicated amount of time. Right: Densitometry of Western blots calculated at the 15-min time point represents three independent experiments, and relative abundance is normalized to the IL-22 alone treatment condition. **(E and G)** IL-1β enhances STAT3 phosphorylation in vivo. Western blot analysis of pSTAT3 and total STAT3 protein of whole cell lysates from colons of (E, left) WT, (G, top) IL-1R$^{fl/fl}$, or IL-1R$^{\Delta IEC}$ mice injected i.p. with IL-1β (100 ng/mouse), IL-22 (50 µg/mouse), or both for 30 min. Densitometry of Western blots represents three independent experiments done on organoids derived from biological triplicates or tissues from three independent mice, and relative abundance is normalized to the IL-22 alone treatment condition (E, right; G, bottom). **(F)** Indicated gene transcripts were quantitated by qPCR of the colon of WT mice injected with IL-22 (50 µg/mouse) or IL-22 + IL-1β (100 ng/mouse) for 1 h. **(H)** Expression of *Reg3g* quantitated by qPCR following IL-1β (100 ng/ml), IL-22 (10 pg/ml), or IL-22 + IL-1β stimulation of mouse colonoids derived from IL-1R$^{fl/fl}$ or IL-1R$^{\Delta IEC}$ mice for 12 h. pSTAT3 represents the phosphorylation of Y705 of STAT3. **(C–G)** Data represent at least three independent experiments (n = 3 mice per group). **(H)** Data represent two independent experiments (n = 3 mice per group). Error bars indicate ± SEM. *P < 0.05, **P < 0.01, ***P < 0.001, and ****P < 0.0001. **(A, B, F, and H)** One-way ANOVA. **(D, E, and G)** Unpaired t tests. US = unstimulated. Source data are available for this figure: SourceData F3.

were induced by IL-22 stimulation (Fig. 4 C). Interestingly, the mRNA sequencing data allowed us to identify that IL-1β stimulation could directly lead to induction of chemokine genes required for immune cell recruitment (*Cxcl1* and *Ccl20*) and ROS/reactive nitrogen species (RNS) production (*Duox2*, *Duoxa2*, *Nos2*, *Nox1*; Fig. 4, E and F).

We next tested if IL-1β stimulation of human spheroids was also capable of inducing chemokines and RNS genes in human cells. The inflammatory mediators induced by IL-22 were enhanced when human rectal spheroids were stimulated with both IL-1β and IL-22 (Fig. 4 G). These results collectively suggest that while IL-1R signaling in colonic epithelial cells of both human and mouse IECs drives the antimicrobial gene program through synergy with IL-22R, it also enhances the production of inflammatory mediators that are induced by IL-22 in human IECs.

Mice deficient for IL-1R expression on IECs are resistant to DSS-induced colitis

Since our sequencing data revealed that IL-1β stimulation of colonoids induced genes associated with ROS production and inflammatory immune cell recruitment, we tested the role of IEC-intrinsic IL-1R in regulating damage induced inflammation. Thus, we used a model of chemically induced acute colitis by administering the detergent DSS into the drinking water of mice (Eichele and Kharbanda, 2017). Mice were given DSS in water ad libitum for 8 d to induce colitis. While *C. rodentium* infection led to more pathology, unexpectedly, we found that IL-1R$^{\Delta IEC}$ mice developed considerably less severe disease when compared to the IL-1R$^{fl/fl}$ littermate controls (Fig. 5). At steady state, the colons of IL-1R$^{fl/fl}$ and IL-1R$^{\Delta IEC}$ mice looked comparable in length (Fig. 5 A). In contrast, IL-1R$^{\Delta IEC}$ mice had longer colons compared to IL-1R$^{fl/fl}$ littermates after 8 d of DSS treatment, indicating they are less affected by the acute inflammation (Fig. 5 A). While the data did not reach statistical significance, we found that IL-1R$^{\Delta IEC}$ mice consistently lost less weight compared to their littermate controls (Fig. S4 A). H&E-stained colons of DSS-treated mice revealed that crypt loss and infiltrating immune cells were much less severe in IL-1R$^{\Delta IEC}$ mice compared to their littermate controls (Fig. 5 B). The IL-1R$^{\Delta IEC}$ mice had less severe diarrhea that developed later than IL-1R$^{fl/fl}$ mice, and differences in rectal bleeding were also apparent between the two groups, with IL-1R$^{\Delta IEC}$ mice displaying significantly lower scores of bleeding and disease scores relative to IL-1R$^{fl/fl}$ littermates (Fig. S4 B). The bulk RNA sequencing revealed IL-1β induced expression of chemokines that recruit neutrophils, and the histology indicates less severe immune cell infiltration; thus we wanted to understand the role of IL-1R signaling on IECs in recruitment of inflammatory cells during DSS colitis. We found that by day 3 of DSS administration the IL-1R$^{fl/fl}$ mice showed increased total number of neutrophils in the lamina propria (Fig. 5 C). Interestingly, we did not observe a change in inflammatory monocyte infiltration (Fig. S4 C) suggesting that their recruitment might be induced by chemokines induced in an IL-1R–independent manner. The infiltration of neutrophils became more apparent by day 5 along with an increase in expression of Ly6G protein and *Ly6g* transcript (a marker for neutrophils) in the colonic tissue (Fig. 5 C and Fig. S4 D). The expression of *Cxcl1* (neutrophil chemokine) and *Duoxa2* (required for ROS production) trended toward being higher in IL-1R$^{fl/fl}$ compared to IL-1R$^{\Delta IEC}$ mice and *Nos2* (required for RNS production) had significantly higher expression in IL-1R$^{fl/fl}$ mice (Fig. 5 D). These results indicate IEC-intrinsic IL-1R signaling contributes to pathology caused by DSS-mediated colitis by upregulating ROS in epithelial cells in addition to inducing expression of chemokines that recruit neutrophils.

Discussion

The intestine houses numerous microbes, and tightly regulated defenses are required to maintain a healthy relationship with the host. However, there is a gap in understanding how various responses by the intestinal epithelium are regulated to maintain homeostasis with commensal microbiota and to initiate appropriate response to invasive intestinal pathogens. In this study, we have identified IL-1R to be crucial for optimal functioning of IECs. Specific deletion of IL-1R on IECs abrogates the ability of small intestinal epithelial cells to produce a wide range of AMPs and clear the intestinal pathogen *C. rodentium*. On the other hand, deletion of IL-1R on IECs led to less severe pathology from inflammation during acute chemical-induced colitis.

It has been proposed by various studies that the ability of the IECs to directly sense microbes or microbial products is critical

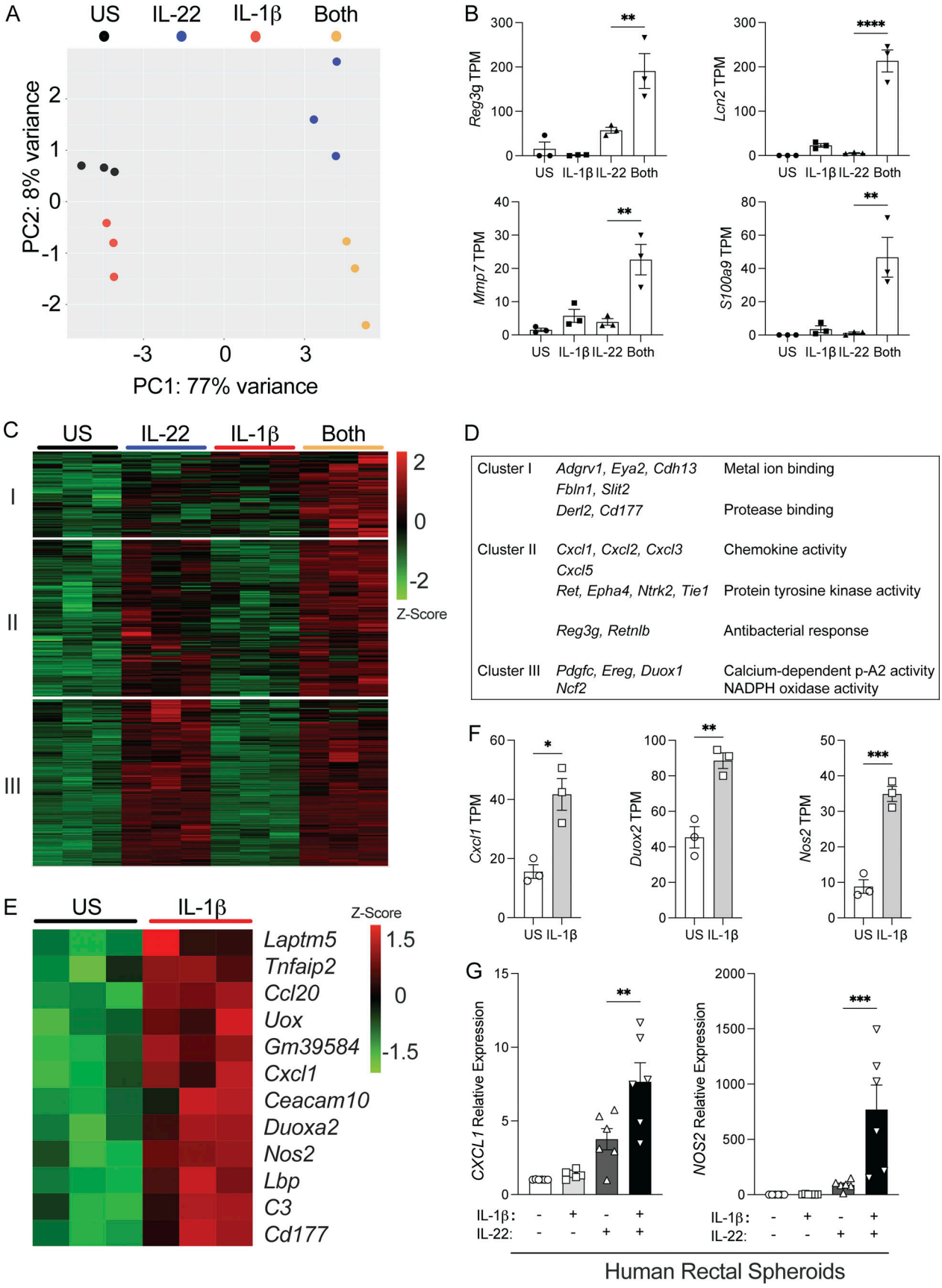

Figure 4. **IL-1β and IL-22 drives distinct IEC transcriptional programs. (A–E)** Transcriptional profiling of mouse colonoids reveals IL-1β synergizes with IL-22 to induce a unique gene profile. **(A)** Principal component analysis of whole transcriptome of colonoids after a 12-h stimulation with IL-1β (100 ng/ml), IL-22

(1 ng/ml), or a combination of both. **(B)** TPM values of antimicrobial genes from clusters II and III that show synergy between IL-1β and IL-22 induced signaling. **(C)** Heatmap of differentially expressed genes in colonoids stimulated with IL-1β, IL-22, or both indicating four clusters of genes. $Log_2FC > 1.0$, false discovery rate < 0.1. **(D)** Functional annotation enrichment of genes in each cluster analyzed by EnrichR. **(E)** Heatmap of differentially expressed genes in mouse colonoids that are induced by IL-1β. **(F)** TPM values of inflammatory genes that are induced by IL-1β in mouse colonoids, as shown in E. **(G)** Expression analysis of indicated genes following stimulation of human rectal spheroids. Indicated gene transcripts were quantitated by qPCR in rectal derived spheroids from six independent healthy human donors stimulated for 12 h using IL-1β (100 ng/ml), IL-22 (1 ng/ml), or a combination of both. Error bars indicate ± SEM. **(A–C, E, and F)** US = unstimulated. **(A–F)** Each data point indicates one biological replicate (n = 3 mice per group). Data in G represent two independent experiments (n = 6 mice per group). *P < 0.05, **P < 0.01, ***P < 0.001, and ****P < 0.0001. **(B and G)** One-way ANOVA. **(F)** Unpaired t test.

to intestinal homeostasis (Rakoff-Nahoum et al., 2004; Menendez et al., 2013; Okumura and Takeda, 2018; Hoytema van Konijnenburg et al., 2017). More specifically, TLR activation in IECs has been implicated in resistance to damage induced by chemicals such as DSS (Rakoff-Nahoum et al., 2004), in mediating interaction between epithelial cells and IELs (Hoytema van Konijnenburg et al., 2017; Ismail et al., 2011), and in antimicrobial peptide production (Frantz et al., 2012; Bhinder et al., 2014; Vaishnava et al., 2008). However, the idea of IECs directly sensing extracellular microbes is rather paradoxical. Since ligands produced by commensal microbes also engage TLRs, constant presence of functional TLRs on IECs would create a persistent state of inflammation that would be detrimental to host homeostasis. At steady state, some species of commensal bacteria tightly associate with the epithelial layer (Atarashi et al., 2015; Ivanov et al., 2009), yet host cells predominantly tolerate microbial presence in the intestinal lumen (Macpherson and Uhr, 2004). Thus, IECs armed with cell surface pattern recognition receptors such as TLRs would also be unable to distinguish between commensal non-virulent and invasive virulent microbes. Since virulent microbes are inherently invasive, it would be more beneficial for IECs to either sense microbes using cytosolic sensors or respond to cues originating from the myeloid and lymphoid cells which are resident in the underlying lamina propria (Lei-Leston et al., 2017; Chen et al., 2008; Kobayashi et al., 2005).

In the past few years, multiple immune-IEC axes were identified. $CD103^+$ DCs and $CX3CR1^+$ macrophages in the lamina propria respond to signals from the luminal content and produce IL-23, which then induce propagation of ILC3s and Th17 cells and induce their production of IL-22 (Muzaki et al., 2016; Parks et al., 2016). IL-22 can directly signal to epithelial cells to produce AMPs (Parks et al., 2016). Additionally, innate immune system derived IL-18 has been implicated in directly inducing goblet cells to produce AMPs (Nowarski et al., 2015). Here, we demonstrate an indispensable role for IL-1R on IECs for maintaining intestinal AMP production. Interestingly, although IL-1R–deficient animals have a severe defect in intestinal AMP levels, IL-1R signaling alone does not induce AMP. We identified a novel function of IL-1R signaling, which serves to synergize with IL-22R signaling and enhance early STAT3 phosphorylation to augment AMP induction in IECs (Fig. S5). This is consistent with IL-1's role to synergize with IL-6, another STAT3 activator, to induce acute phase response in the liver and in driving optimal mucosal CD4 T cell responses (Whitley et al., 2018; Deason et al., 2018). It was perplexing that in $IL\text{-}1R^{\Delta IEC}$ mice injection of both IL-1β and IL-22 led to decreased pSTAT3 compared to IL-22 injection alone. This could perhaps be a result of IL-1β functioning on another cell type to induce negative regulators such as IL-22–binding protein leading to reduced activity of IL-22, and this outcome is only apparent in the absence of IL-1R on IECs. Lastly, we found that mice deficient for IL-1R on IECs are unable to clear the intestinal pathogen *C. rodentium*. It is important to note here that while $IL\text{-}1R^{\Delta IEC}$ mice had reduced AMP expression at steady state, infection by *C. rodentium* lead to robust induction of both *Reg3g* and *Lcn2*, suggesting that the early burst of IL-22 bypasses the need for IL-1R signaling. When IL-22 levels drop, which is likely to happen during later stages of the infection, there appears to be an obligatory need for IEC-intrinsic IL-1R signaling to maintain the AMP production. Interestingly our results also revealed that IL-1β can induce gene expression of chemokines in IECs that would recruit neutrophils which actively participate in pathogen clearance (Fig. 4 E; Spehlmann et al., 2009). Thus, the inability of $IL\text{-}1R^{\Delta IEC}$ mice to clear *C. rodentium* could be a combination of defects in *Reg3g* expression at late stages of infection along with other defects such as induction of chemokines and genes involved in ROS production. Future studies will be required to elucidate the exact role of IEC-intrinsic IL-1R signaling in clearance of intestinal pathogens.

The use of $IL\text{-}1R^{-/-}$ or $IL\text{-}1R^{\Delta IEC}$ mice does not provide insights into the nature of the specific IL-1 family signal that is responsible for inducing AMPs. Further studies will be required to understand if IECs sense IL-1α or IL-1β to induce gene synthesis, especially because these cytokines are produced in vastly different ways. Although inflammasome-mediated caspase-1 activation by commensal microbes has been shown to be largely responsible for production of IL-1β in the intestines (Seo et al., 2015), production of IL-1α can be because of cell death and extracellular proteolytic cleavage (Di Paolo and Shayakhmetov, 2016; Lopez-Castejon and Brough, 2011). Thus, we speculate that either IL-1α produced from cells turning over in the intestines or low-level inflammasome activation in lamina propria myeloid cells sensing some commensals might largely dictate AMP response at steady state. However, during active intestinal infections, IL-1β, produced by lamina propria myeloid cells in response to microbe-induced inflammasome activation, might drive a more robust AMP response by its direct action on epithelial cells as well as through IL-22 production by Th17 cells and ILC3s (Coccia et al., 2012). The detrimental role we found during acute inflammation could be more related to IL-1α, that would be released due to tissue damage and cell death (Menghini et al., 2019). Here we propose a dynamic, site-specific function for IEC-intrinsic IL-1R signaling. At steady state, IL-1 drives an antimicrobial program in IECs. In the event of epithelial barrier disruption, however, it appears to have a damaging role due to induction of inflammatory mediators. Previous studies have

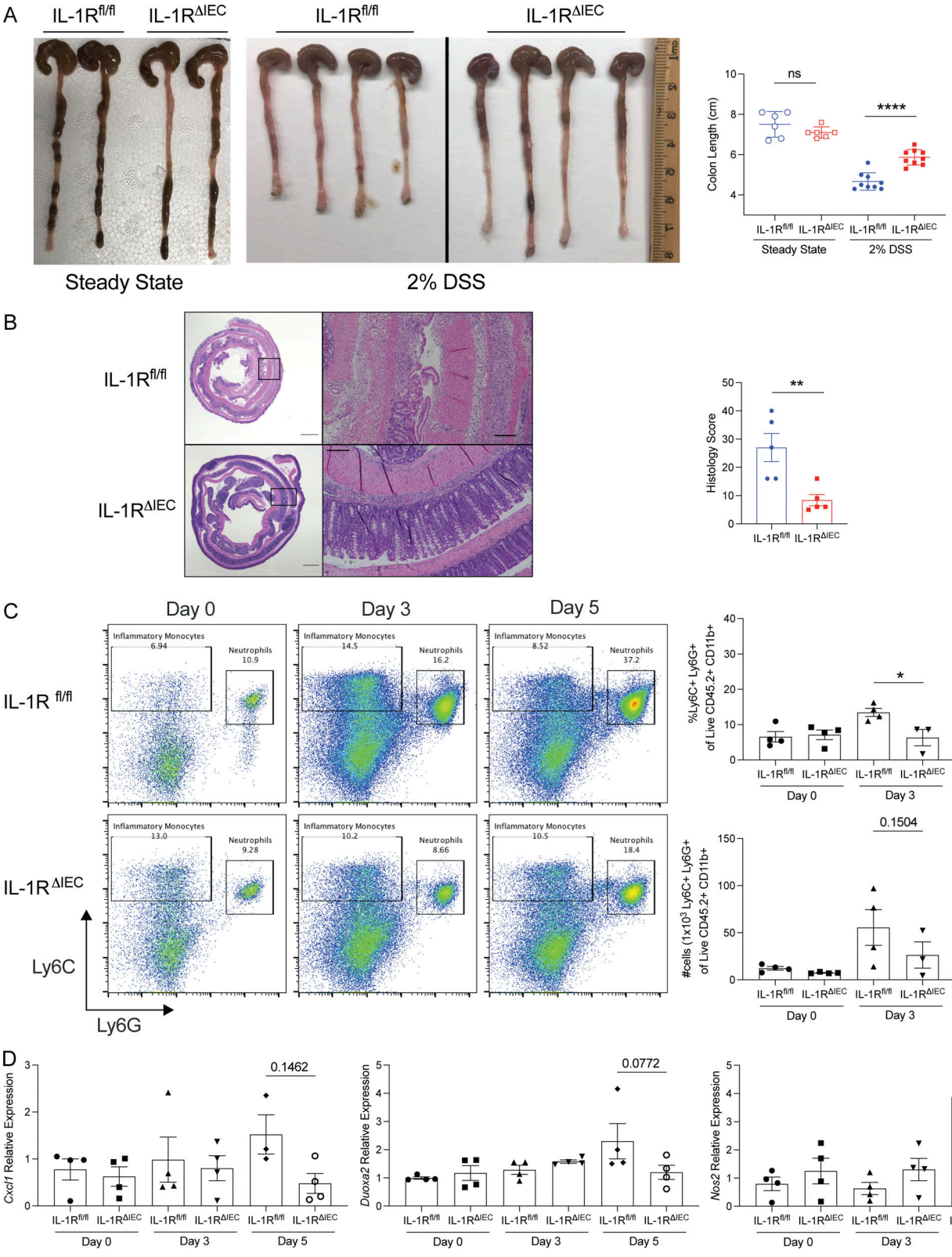

Figure 5. **Mice lacking IL-1R expression on IECs are resistant to DSS-induced colitis. (A)** Representative image of colons and their quantified lengths at steady state or from IL-1R$^{fl/fl}$ (n = 12) and IL-1R$^{\Delta IEC}$ (n = 12) mice given a 2% DSS solution in drinking water for 8 d. **(B)** Representative images of histopathological changes in colon tissue by H&E staining after day 8 of 2% DSS given to IL-1R$^{fl/fl}$ and IL-1R$^{\Delta IEC}$ mice and histological score of the pathology (n = 5 colons per group). Scale = 1,000 µm (left panels) and 200 µm (right panels). **(C)** Flow cytometry of lamina propria cells showing inflammatory monocyte (Ly6C$^+$ Ly6G$^-$) and neutrophil infiltration (gated on Live CD45.2$^+$ CD11b$^+$ cells—neutrophils considered Ly6G$^+$ Ly6C int population) at steady state (day 0), day 3, and day 5 after administration of 2% DSS in drinking water. **(D)** Expression analysis by qPCR of indicated genes in colon tissue of mice at steady state (day 0) or given 2% DSS in drinking water for 3 or 5 d. All mice were littermates in cages containing at least two mice of each genotype. Data represent three independent experiments. Error bars indicate ± SEM. *P < 0.05, **P < 0.01, and ****P < 0.0001. **(A–D)** Unpaired t test.

found that *Il1r1* has three different promoters (Chen et al., 2009). Thus, it is possible that depending on cell type and location, different promoters regulate IL-1R expression and signaling. It is very well known that there are significant changes in immune cells and epithelial cell types throughout the entire intestine (Mowat and Agace, 2014). Interestingly, we found that IL-1R is expressed at higher levels in the colon, and we observed stronger IL-1R/IL-22R synergy in colonoids compared to enteroids, supporting this idea (Fig. 3, A and C; and Fig. S3 B).

The role of IL-1R signaling during inflammatory disease is quite controversial (Coccia et al., 2012; González-Navajas et al., 2010; Seo et al., 2015). Most studies used whole body deletion of IL-1R or systemic IL-1β neutralization to study the role of IL-1R signaling in intestinal inflammation (Villeret et al., 2013; Krysko et al., 2013; Carvalho et al., 2012; Yoshida et al., 2010); however, various cell types including epithelial cells, innate, and adaptive immune cells express and engage IL-1R signaling (McEntee et al., 2019). Thus, by global depletion of IL-1R or the downstream signaling components, it is impossible to interpret the contributions of cell-specific responses. A previous study, for example, demonstrated that IL-1R KO mice are highly susceptible to *C. rodentium* infection as revealed by increased predisposition to intestinal damage in addition to increased pathology following 14 d of DSS administration (Lebeis et al., 2009). Since sensing of IL-1 by Th17 cells and ILC3s is critical for IL-22 production, which in turn regulates antimicrobial responses and repair, it is difficult to ascertain the contribution of IEC-specific IL-1R signaling to the observed outcomes. Here we showed that specifically deleting IL-1R on IECs provided protection against DSS-induced colitis, revealing the damaging role of hyper–IL-1R signaling in IECs (Fig. S5). We found deletion of IL-1R on IECs resulted in impaired recruitment of neutrophils and impaired expression of genes associated with ROS or RNS production. Inflammatory cell recruitment contributes to damage caused by inflammation, and oxidative stress induced ROS/RNS have been found to be detrimental to the host during acute inflammation (Bourgonje et al., 2020; Wéra et al., 2016). We suspect that IL-22 in the DSS model would be playing a role in tissue repair, which we do not propose is linked the defective IL-1R signaling in the IL-1R$^{\Delta IEC}$ mice. Further studies will be needed to elucidate the specific contribution the IL-1R–chemokine/ROS/RNS pathway, as well as IL-22, has in the pathogenesis of intestinal inflammation. Studies that find full body deletion of IL-1R to be harmful could be a result of loss of function in ILC3s and Th17s which respond to IL-1β to produce IL-22 (Jain et al., 2018; Klose and Artis, 2016). Additionally, deletion of MyD88 would be harmful to the host because myeloid cells would lose the capacity to respond to microbial ligands through the TLR signaling pathway. There would be defective phagocytosis, and a lack of clearance of any commensal bacteria that get across the epithelium in addition to impaired IL-1R signaling pathway due to lack of upregulation of inflammasome machinery and production of IL-1β (Song et al., 2018b; Gasse et al., 2007; Marr et al., 2003). Thus, our investigation specifically teases out the function of IEC-intrinsic IL-1R signaling allowing us to conclude that it contributes to pathology during acute inflammatory colitis.

Various studies demonstrated that epithelial ROS production is critical for intestinal defense against several microbes (Aratani, 2018; Staerck et al., 2017; Rhen, 2019; Dryden, 2018). Additionally, low levels of ROS are required at homeostasis for intracellular signaling and wound repair in IECs (Lipinski et al., 2009; Leoni et al., 2015). However, during inflammatory conditions, such as inflammatory bowel disease (IBD), exuberant ROS production and accumulation cause cell death and tissue pathology (Zhao et al., 2018; MacFie et al., 2014; McKenzie et al., 1996; Hayes et al., 2015). In this study, we found that IL-1R signaling on IECs contributes to ROS-gene induction, which could contribute to tissue damage and exacerbate disease pathology during DSS-induced colitis. Additionally, the synergy between IL-1β and IL-22 that we discovered in mouse epithelial cells was also present in human colonic epithelial cells. In fact, we observed synergy between IL-1β and IL-22 in human cells that enhanced *NOS2* and *CXCL1* expression (Fig. 4 G). This has major implications since it implies IL-22R could be playing a pathogenic role in inflammatory responses in the gut due to its ability to synergize with IL-1R signaling. These findings agree with past studies that find higher levels of IL-22 associated with Crohn's disease (Brand et al., 2006), and we propose that IL-22 has a detrimental role in IBD due to its ability to drive inflammatory gene expression and immune cell migration by acting synergistically with IL-1. Previous reports have found mixed results when treating IBD patients with anti–IL-1β treatments such as Anakinra (Cavalli and Dinarello, 2018; Mao et al., 2018; Hügle et al., 2017). However, these confounding results are not surprising given the previously described broad function of IL-1R on various cell types involved in intestinal immune responses. Thus, designing IEC-targeted IL-1R blockage strategies or combined blockade of IL-22 and IL-1R could specifically reduce tissue oxidative stress and pathology and serve as an effective treatment for IBD.

Materials and methods

Mice

C57BL/6 WT control mice were obtained from the University of Texas (UT) Southwestern Mouse Breeding Core Facility or bred internally in a specific pathogen–free facility at Cincinnati Children's Hospital Medical Center. *Il1r1*$^{-/-}$ mice were purchased from The Jackson Laboratory. *Il1r1*$^{fl/fl}$ mice were a gift from Randy Blakely, Vanderbilt University, and crossed to B6.Cg-Tg(Vil1-cre)997Gum/J mice purchased from The Jackson Laboratory. The *Il1r1* globally restored *Il1r1*$^{GR/GR}$ mice were a gift from Ning Quan, Florida Atlantic University. All mice were bred and housed in a specific pathogen–free facility at UT Southwestern Medical Center or Cincinnati Children's Hospital Medical Center. All mouse experiments were done as per protocols approved by Institutional Animal Care and Use Committee at UT Southwestern Medical Center and Cincinnati Children's Hospital Medical Center.

Bacterial strains and infections

C. rodentium (Cr: strain ICC168, nalidixic acid-resistant) were cultured in agar plate of Luria-Bertani, with 30 μg/ml nalidixic

acid. A single colony was chosen and secondarily expanded in the respective liquid broth with appropriate antibiotics. Bacteria were grown to log phase (OD_{600} = 0.6–1) on the day of infection, extensively washed, and resuspended in PBS. Mice that had food removed for 12 h prior were orally gavaged 1% sodium bicarbonate and, 15 min later, infected with 2 × 10^9 CFU of *C. rodentium* by oral gavage.

Extraction of *C. rodentium* lysates and protein quantification

Bacterial cultures were grown to late log phase (OD_{600} = 0.8–1.2), washed extensively, and resuspended in PBS. Suspensions were subjected to three cycles of snap freeze and thaw in liquid nitrogen and under running room-temperature water. Then the suspension was lysed by repeated probe sonication (Qsonica Sonicator) at a duty cycle 30% for a total of five to six cycles of 30 s on, 30 s off. Complete lysis was determined by the visible clearance of the suspension and achievement of maximum protein concentration as measured by Bradford Assay Kit (Bio-Rad). Lysates were centrifuged at 4,000 rpm for 20 min to remove insoluble components. Supernatants are then sterilized through a 0.22 µm membrane filter. Protein concentration of the lysate is estimated by Pierce BCA Protein Assay Kit (Thermo Fisher Scientific).

DSS-induced colitis

Acute colitis was induced with 2% (wt/vol) DSS (molecular mass 36–40 kD; MP Biologicals) dissolved in distilled water and filtered. DSS was administered ad libitum in the drinking water for 3–8 d. Body weight, stool consistency, and the presence of occult blood were determined daily. The scoring system was determined before the start of the experiments. Stool scores were as follows: 0, pellets that are dry/crumble when smashed with moderate force; 1, pellets that have form, appear moist, and smear when smashed with moderate force; 2, wet pellets with minor form that adhere to the sampling stick when touched and require very minor force to smear; 3, liquid stools/stools with no form and require no force to smear. Bleeding scores were determined as follows: 0, no blood as tested with ColoScreen (Thermo Fisher Scientific); 1, positive hemoccult; 2, blood traces in stool visible; 3, gross rectal bleeding.

Generation of murine enteroids and colonoids

Mouse ileum or colons were dissected and flushed with ice-cold PBS. The ileum or colon was opened longitudinally, cut into 1-cm pieces, and incubated in 2 mM EDTA for 30 min at 4°C with rocking. The tissue was transferred into a new tube containing 5 ml of shaking buffer (PBS, 43.3 mM sucrose, 54.9 mM sorbitol) and shaken gently by hand for 2 min. Dispersed crypts were plated overnight in Matrigel (Corning) with enteroid growth media (Advanced DMEM/F12, 2 mM GlutaMax, 10 mM Hepes, 100 U/ml penicillin, 100 µg/ml streptomycin, 1× N2 supplement, 1× B27 supplement [all from Invitrogen]) containing epidermal growth factor (EGF; 50 ng/ml; Sigma-Aldrich), 40% L-WRN conditioned media (L-WRN cells from American Type Culture Collection), and 10 µM Y-27632 (ROCK inhibitor; Tocris Bioscience, R&D Systems). The mouse spheroids were then stimulated with mouse recombinant IL-1β (100 ng/ml; PeproTech) and recombinant mouse IL-22 (1 ng/ml for colonoids, 10 pg/ml for enteroids; BioLegend; Table 1) for 15 min to 12 h depending on the experiment.

Table 1. **Recombinant cytokines used for in vivo and in vitro experiments**

Target	Company	Ref #
Mouse IL-22 (in vitro)	R&D	582-ML-010
hIL-22.Fc protein (in vivo)	Genentech	
Mouse IL-1β	PeproTech	211-11B
Human IL-22	PeproTech	200-22
Human IL-1β	PeproTech	200-01B

Generation of human spheroids

Human rectal spheroid lines were previously established from biopsy tissues of six adult donors collected during routine endoscopic procedures and maintained in three-dimensional culture by embedding in Matrigel Matrix (Corning 354234; 15 µl/well) and providing 50% L-WRN conditioned medium (L-WRN CM) supplemented with 10 µM Y-27632 (ROCK inhibitor; Tocris Bioscience, R&D Systems) and 10 µM SB 431542 (TGFBR1 inhibitor; Tocris Bioscience, R&D Systems), as previously described (VanDussen et al., 2015; VanDussen et al., 2019). Briefly, for cytokine stimulation experiments, spheroids were passaged using 1× trypsin in 0.5 mM PBS-EDTA, resuspended in Matrigel, and provided 400 µl of 50% L-WRN CM supplemented with 10 µM Y-27632 and 10 µM SB 431542 overnight to recover spheroids. The following day, L-WRN CM was aspirated, wells were washed with PBS, and provided differentiation media (Miyoshi et al., 2017; Advanced DMEM/F-12 [Invitrogen] supplemented with 2 mM *L*-glutamine, 100 U/ml penicillin, 0.1 mg/ml streptomycin, 50 ng/ml EGF [PeproTech], 10 µM Y-27632, and 10 µM L-161,982 [EP4 inhibitor, R&D Systems]) for 24 h. Differentiated rectal spheroids were then stimulated for 12 h with human recombinant IL-1β (100 ng/ml; PeproTech) and human recombinant IL-22 (1 ng/ml; BioLegend) in differentiation medium. This study was approved by the Cincinnati Children's Hospital Medical Center Institutional Review Board.

Histopathology

To assess epithelial IL-1R expression, ileal and colon tissues from the *Il1r1*$^{GR/GR}$ reporter mice were excised and fixed in 4% paraformaldehyde overnight, washed in 20% sucrose, and embedded in OCT. Frozen tissue sections (8 µm) were immunostained by blocking in 1% BSA in 1% Triton X-100 in PBS followed by incubation with primary rat antibody E-Cadherin (clone ECCD-2, 1:200; 13-1900; Invitrogen) and donkey anti-rat secondary antibody conjugated to AlexaFluor488 (1:500; Jackson ImmunoResearch). Nuclei were stained with Hoechst 33258 (Invitrogen). Coverslips were mounted with ProLong Gold (Invitrogen). Images were taken at 20× using an upright Nikon 90i motorized microscope and Andor Zyla 4.2 SCMOS cooled monochrome camera with Nikon NIS elements v.5 software. Brightness,

contrast, and hue (for blue channel only) were adjusted in Adobe Photoshop 2021.

To assess the role of IL-1R in intestinal injury, after day 8 of DSS or day 37 of *C. rodentium* infection, the entire colon was excised to measure the length of the colon. Colons were washed, fixed in 10% normal buffered formalin, and embedded in paraffin. Tissue sections were stained with H&E for histological analysis. Slides were imaged at 10×, 20×, or 40× using a DM2000 Compound Research Photomicroscope (Leica). Colon tissues from DSS colitis experiments were scored in a double-blinded fashion by the following parameters: Severity of inflammation (0–3), depth of injury/inflammation (0–3), and crypt damage (0–4). DSS histological scores were multiplied by a factor representing the percentage of tissue involvement: ×1 (0–25%), ×2 (26–50%), ×3 (51–75%), and ×4 (76–100%). Thus, the maximum colitis score in the DSS model is 40 (Krieglstein et al., 2007).

Isolation of IECs, quantitative PCR (qPCR), and flow cytometry

Small intestine and colons were harvested from mice, flushed with PBS, cut open longitudinally, and incubated with EDTA and 1 mM DTT for 30 min at 4°C on a rocker. Supernatants were then passed through a 100-micron filter and centrifuged at 500 ×*g* for 5 min. For RNA, IECs were then resuspended in Trizol, homogenized by passing repeatedly through a 25-gauge needle, and stored at −80°C until RNA was isolated. Total RNA was isolated from small intestinal tissues by homogenizing with an OMNI homogenizer with soft tissue tips in RLT buffer (from Qiagen) + β-mercaptoethanol. All RNA was isolated by using Qiagen RNeasy RNA Isolation Kits according to the manufacturer's protocol and were used to synthesize cDNA. PowerUp SYBR Green Master Mix and specific primers were used for qPCR (Table 2 and Table 3). Signals were normalized to *Hprt1* levels within each sample using published primers (Irizarry-Caro et al., 2020) and normalized data were used to quantitate relative levels of gene expression using ΔΔCt analysis. For flow cytometry, IECs were then blocked with Fc block (anti-mouse CD16/CD32; BioLegend) for 10 min and then incubated with antibodies for 30 min (Table 4), with extensive washes with FACS buffer (PBS, 2%FCS, 2 mM EDTA) in between. Before running, IECs were passed through a tube-top 35-micron filter. Samples were analyzed using LSR II flow cytometer (BD) or Novocyte 3001 (ACEA Biosciences). Cells were gated on singlets and dead cells were excluded using Zombie Yellow Live/Dead staining (BioLegend). Data were analyzed using FlowJo software (BD). Purity of IEC isolations were repeatedly assessed and were consistently 95–99% CD45-IECs.

RNA sequencing analysis

Mouse colonoids were stimulated with mouse recombinant-IL-1β (100 ng/ml), mouse recombinant IL-22 (1 ng/ml), or both for 12 h. RNA was isolated by using Qiagen RNeasy RNA Isolation Kits according to the manufacturer's protocol. RNA sequencing libraries were prepared with the Illumina TruSeq Stranded RNA Sample Preparation kit (Illumina) according to the manufacturer's protocol. Quality of the libraries was validated on an Agilent Bioanalyzer 2100. This included using standard protocols for cDNA synthesis, fragmentation, addition of adaptors, size selection, amplification, and quality control (Illumina). The amplified libraries were size-selected, and libraries were quantified by PicoGreen assay (Life Technologies). SE85 single-end sequencing was performed using NextSeq SE-75 High Output V2 flow cell with an average of 20 million reads/sample. Alignment of RNA sequencing reads on mouse reference genome mm10

Table 2. **Primers used for qPCR amplification of mouse genes**

Mouse		
Reg3g	Forward 5′–3′:	5′-TTCCTGTCCTCCATGATCAAAA-3′
	Reverse 5′–3′:	5′-CATCCACCTCTGTTGGGTTCA-3′
Reg3b	Forward 5′–3′:	5′-TACTGCCTTAGACCGTGCTTTCTG-3′
	Reverse 5′–3′:	5′-GACATAGGGCAACTTCACCTCACA-3′
Saa1	Forward 5′–3′:	5′-CATTTGTTCACGAGGCTTTCC-3′
	Reverse 5′–3′:	5′-GTTTTTCCAGTTAGCTTCCTTCATGT-3′
Il22	Forward 5′–3′:	5′-CAATCAGCTCAGCTCCTGTCACAT-3′
	Reverse 5′–3′:	5′-TCCCCAATCGCCTTGATCTCTCCA-3′
Lcn2	Forward 5′–3′:	5′-AAGGCAGCTTTACGATGTACAGC-3′
	Reverse 5′–3′:	5′-CTTGCACATTGTAGCTGTGTACC-3′
Cxcl1	Forward 5′–3′:	5′-CTGCACCCAAACCGAAGTCAT-3′
	Reverse 5′–3′:	5′-TTGTCAGAAGCCAGCGTTCAC-3′
Duoxa2	Forward 5′–3′:	5′-GCCTGGCTTTGCTCACCA-3′
	Reverse 5′–3′:	5′-GAGGAGGAGGCTCAGGAT-3′
Nos2	Forward 5′–3′:	5′-CACCTTGGAGTTCACCCAGT-3′
	Reverse 5′–3′:	5′-ACCACTCGTACTTGGGATGC-3′
Il1r1	Forward 5′–3′:	5′-TGAGTTACCCGAGGTCCAGT-3′
	Reverse 5′–3′:	5′-GCTTCCCCCGGAACGTATAG-3′
Epcam	Forward 5′–3′:	5′-AGGGGCGATCCAGAACAACG-3′
	Reverse 5′–3′:	5′-ATGGTCGTAGGGGCTTTCTC-3′
Ly6g	Forward 5′–3′:	5′-GAGAGGAAGTTTTATCTGTGCAGCC-3′
	Reverse 5′–3′:	5′-TCAGGTGGGACCCCAATACA-3′
Hprt1	Forward 5′–3′:	5′-CAGTCCCAGCGTCGTGATTA-3′
	Reverse 5′–3′:	5′-TGGCCTCCCATCTCCTTCAT-3′

Table 3. **Primers used for qPCR amplification of human genes**

Human		
REG3A	Forward 5′–3′:	5′-ACCATATCCCACCAGAGAGTGA-3′
	Reverse 5′–3′:	5′-TCACCTTGAACCTGAGACAGC-3′
LCN2	Forward 5′–3′:	5′-TTCCCTGTCCCAATCGACCA-3′
	Reverse 5′–3′:	5′-TTTAGCAGACAAGGTGGGGC-3′
S100A9	Forward 5′–3′:	5′-CTGCAAAATTTTCTCAAGAAGGAGA-3′
	Reverse 5′–3′:	5′-CACCCTCGTGCATCTTCTCG-3′
CXCL1	Forward 5′–3′:	5′-CTGGCTTAGAACAAAGGGGCT-3′
	Reverse 5′–3′:	5′-TAAAGGTAGCCCTTGTTTCCCC-3′
NOS2	Forward 5′–3′:	5′-CGCATGACCTTGGTGTTTGG-3′
	Reverse 5′–3′:	5′-CATAGACCTTGGGCTTGCCA-3′

Table 4. **Antibodies used for flow cytometry and immunofluorescent histology**

Target	Clone	Company	Ref #
Mouse E-Cadherin	4A2	CST	14472
DAPI	N/A	BioLegend	422801
CD45.2 FITC	104	BioLegend	109806
CD90.2 BV785	30-H12	BioLegend	105331
CD11b PE	M1/70	BioLegend	101208
Ly6C BV711	HK1.4	BioLegend	128037
Ly6G APC	1A8	BioLegend	127614
CD45.2 AF700	104	BioLegend	109822
EpCAM BV711	G8.8	BioLegend	118233

was performed on CLC Genomics Workbench 7 (Qiagen). The expression of the genes in all samples was calculated as Reads Per Kilobase of Transcripts Per Million mapped reads (TPM). Differential gene expression between groups were evaluated using DESeq2 (Love et al., 2014). Heatmaps of genes were generated in R using ggplot2 (Wickham, 2016). RNA sequencing data are publicly available (GSE193267).

Shotgun metagenome sequencing

DNA was extracted from one or two fecal pellets using the Power Fecal DNA Isolation Kit by MO BIO per kit instructions. DNA concentration was measured using Qbit. Amplified library generation was performed using the Nextera XT protocol according to the manufacturer's recommendations, and sequencing was performed to obtain 150 bp DNA paired end reads to a depth of ∼20 million base pairs per sample using an Illumina NovaSeq 6000 sequencing machine (Illumina Corp.)

Shotgun sequencing data analysis

Raw sequence reads were extracted and demultiplexed using the Illumina program bcl2fastq. Raw reads were then filtered and trimmed for quality control using the program Sickle (Joshi and Fass, 2011). Trimmed reads were aligned using Kraken (Wood and Salzberg, 2014) to a custom microbial genome database (that includes all RefSeq bacterial, fungal, parasitic, and viral genomes supplemented with additional bacterial and fungal genome sequences from the National Center for Bioinformatics [NCBI] to determine quantitative genus and species abundance for more than 40,000 microbial species genomes). An exact sequence read match of k-mer length 32 was used in Kraken to assign reads to the lowest common ancestor. Normalization of count data to the lowest number of total reads mapped among the samples was performed using rrarefy with the Vegan package in R to give the relative abundance at both the genus and species level (Oksanen et al., 2015). Principal component analysis was performed on a Euclidian distance matrix calculated from normalized species abundance data using the ade4, Vegan, and FactoExtra packages in R and the FactoExtra package. Statistical significance of differences in overall microbiome composition were determined using multiresponse permutations procedures, a form of PERMANOVA (Xia and Sun, 2017). Differential species and genus abundance between groups was determined by pairwise Wilcox rank sum test with false-discovery rate correction for multiple testing. Fold-change (FC) and $\log_2$FC were calculated with the gtools package in R. Stool samples at all time points between the patients with normal and abnormal intestinal permeability were grouped for comparison.

Western blot analysis

Whole cell lysates were obtained from small intestine and colon tissue by flushing tissue with ice-cold PBS, then cutting longitudinally into 1-cm pieces. Pieces were then placed in high impact 2 ml tubes along with five metal lysing beads (MP: 116925000) and 500 µl of 1× radioimmunoprecipitation assay buffer containing phosphatase and protease inhibitors. Tubes were shaken using a TissueLyser (Qiagen) at a frequency of 30/s for 3 min. Cells from mouse organoids were extracted from Matrigel using Cell recovery solution (Corning: 354253) at a 1:2 ratio and then incubated at 4°C for 10 min. Cells were then centrifuged at 450 ×*g* for 5 min in a 96-well round-bottom plate and the Matrigel Cell recovery solution was flicked off. Cells were lysed in 1× radioimmunoprecipitation assay buffer containing phosphatase and protease inhibitors for 5 min on ice. All protein was quantified using Pierce BCA Protein Assay Kit. Cell lysates were boiled in 1× Laemmli buffer at 95°C for 10 min. Cell lysates were separated by SDS-PAGE and transferred onto polyvinylidene difluoride membranes. Blots were incubated with anti-Stat3 (1:5,000; CST: 9139S), and anti-phospho-Stat3 (pY705; 1:2,000; 612356; Thermo Fisher Scientific). As secondary antibodies, anti-rabbit-IgG-HRP (1706515; Bio-Rad; 1:10,000) and anti-mouse-IgG-HRP (1706516; Bio-Rad) were used. anti-βtubulin (1:5,000; CST 2146S) was used as control. Western blot was developed using SuperSignal West Pico PLUS Chemiluminescent Substrate (34578; Thermo Fisher Scientific) and ECL signal was recorded on X-Ray Films using a developer (Phenix: F-BX810).

ELISA

Capture antibody for IL-17A (BioLegend, TC11-18H10.1) or IL-22 (DuoSet ELISA Kit, R&D) was diluted and used to coat 96-well flat-bottom plates overnight at 4°C. Plates were blocked with PBS containing 10% FBS (IL-17A), or PBS containing 5% Tween (IL-22) for 2 h at room temperature. Samples were diluted in blocking buffer and loaded in duplicate and then incubated overnight at 4°C. Detection antibodies for IL-17A (TC11-8H4; BioLegend) or IL-22 (DuoSet ELISA Kit, R&D) were diluted and used according to standard procedure. Using a standard curve of known concentrations of IL-17A and IL-22, quantities of each cytokine in the supernatant samples were quantified by using o-phenylenediamine dihydrochloride colorimetric assay.

Online supplemental material

Fig. S1 shows additional supporting data regarding the expression of IL-1R on IECs. Fig. S2 provides data on the composition of microbiota in IL-1R$^{fl/fl}$ and IL-1R$^{\Delta IEC}$ mice as well as additional data that demonstrate *C. rodentium* induced pathology in IL-1R$^{\Delta IEC}$ mice. Fig. S3 provides additional characterization of

IL-1R expression on colonoids as well as the synergy between IL-1β and IL-22 to drive AMPs. Fig. S4 provides supporting data that demonstrate the resistance of IL-1R$^{\Delta IEC}$ mice to DSS induced colitis. Fig. S5 provides a model that depicts the dual role of IEC-intrinsic IL-1R signaling in intestinal homeostasis and inflammation.

Data availability

All data are available from the corresponding author upon reasonable request. The data underlying Fig. 4 are openly available at NCBI's Gene Expression Omnibus. The accession number is GSE193267.

Acknowledgments

We thank all the current and former members of the Pasare lab, especially Aakanksha Jain, Margaret McDaniel, and Yajing Gao for their insight, helpful discussions, and critical reading of this manuscript. Special thanks to Jeff Valance for help with microscopy. We thank Randy Blakely (Vanderbilt University, Nashville, TN) for IL-1R floxed mice, and Ning Quan (Florida Atlantic University, Boca Raton, FL) for IL-1R global restore reporter mice. Human FcIL-22 reagent was a gift from Genentech, Inc. Fig. S5 was created by Biorender.com.

This work was supported National Institutes of Health grants R01 AI123176 and R01AI155426 to C. Pasare.

Author contributions: Data curation: H.E. Meibers and D.B. Haslam. Formal analysis: V.G. Jain and D.B. Haslam. Funding acquisition: C. Pasare. Investigation: G. Overcast, E. Eshleman, H.E. Meibers, I. Saha, L. Waggoner, K.N. Patel, and K. VanDussen. Methodology: T. Alenghat and K. VanDussen. Resources: C. Pasare, T. Alenghat, and K. Vandussen. Supervision: C. Pasare. Visualization: G. Overcast, H.E. Meibers, and K. VanDussen. Writing—original draft: G. Overcast, H.E. Meibers, and C. Pasare. Writing—review and editing: G. Overcast, H.E. Meibers, E. Eshleman, T. Alenghat, K. VanDussen, and C. Pasare.

Disclosures: The authors declare no competing interests exist.

Submitted: 20 December 2021
Revised: 20 December 2022
Accepted: 2 March 2023

References

Aratani, Y. 2018. Myeloperoxidase: Its role for host defense, inflammation, and neutrophil function. *Arch. Biochem. Biophys.* 640:47–52. https://doi.org/10.1016/j.abb.2018.01.004

Atarashi, K., T. Tanoue, M. Ando, N. Kamada, Y. Nagano, S. Narushima, W. Suda, A. Imaoka, H. Setoyama, T. Nagamori, et al. 2015. Th17 cell induction by adhesion of microbes to intestinal epithelial cells. *Cell*. 163: 367–380. https://doi.org/10.1016/j.cell.2015.08.058

Bhinder, G., M. Stahl, H.P. Sham, S.M. Crowley, V. Morampudi, U. Dalwadi, C. Ma, K. Jacobson, and B.A. Vallance. 2014. Intestinal epithelium-specific MyD88 signaling impacts host susceptibility to infectious colitis by promoting protective goblet cell and antimicrobial responses. *Infect. Immun.* 82:3753–3763. https://doi.org/10.1128/IAI.02045-14

Bourgonje, A.R., M. Feelisch, K.N. Faber, A. Pasch, G. Dijkstra, and H. van Goor. 2020. Oxidative stress and redox-modulating therapeutics in inflammatory bowel disease. *Trends Mol. Med.* 26:1034–1046. https://doi.org/10.1016/j.molmed.2020.06.006

Brand, S., F. Beigel, T. Olszak, K. Zitzmann, S.T. Eichhorst, J.M. Otte, H. Diepolder, A. Marquardt, W. Jagla, A. Popp, et al. 2006. IL-22 is increased in active Crohn's disease and promotes proinflammatory gene expression and intestinal epithelial cell migration. *Am. J. Physiol. Gastrointest. Liver Physiol.* 290:G827–G838. https://doi.org/10.1152/ajpgi.00513.2005

Burgueño, J.F., and M.T. Abreu. 2020. Epithelial Toll-like receptors and their role in gut homeostasis and disease. *Nat. Rev. Gastroenterol. Hepatol.* 17: 263–278. https://doi.org/10.1038/s41575-019-0261-4

Byndloss, M.X., E.E. Olsan, F. Rivera-Chávez, C.R. Tiffany, S.A. Cevallos, K.L. Lokken, T.P. Torres, A.J. Byndloss, F. Faber, Y. Gao, et al. 2017. Microbiota-activated PPAR-γ signaling inhibits dysbiotic Enterobacteriaceae expansion. *Science*. 357:570–575. https://doi.org/10.1126/science.aam9949

Carvalho, F.A., I. Nalbantoglu, S. Ortega-Fernandez, J.D. Aitken, Y. Su, O. Koren, W.A. Walters, R. Knight, R.E. Ley, M. Vijay-Kumar, and A.T. Gewirtz. 2012. Interleukin-1β (IL-1β) promotes susceptibility of Toll-like receptor 5 (TLR5) deficient mice to colitis. *Gut*. 61:373–384. https://doi.org/10.1136/gut.2011.240556

Cavalli, G., and C.A. Dinarello. 2018. Anakinra therapy for non-cancer inflammatory diseases. *Front. Pharmacol.* 9:1157. https://doi.org/10.3389/fphar.2018.01157

Chen, G.Y., M.H. Shaw, G. Redondo, and G. Núñez. 2008. The innate immune receptor Nod1 protects the intestine from inflammation-induced tumorigenesis. *Cancer Res.* 68:10060–10067. https://doi.org/10.1158/0008-5472.CAN-08-2061

Chen, Q., H. Zhang, Q. Li, Y. An, M. Herkenham, W. Lai, P. Popovich, S. Agarwal, and N. Quan. 2009. Three promoters regulate tissue- and cell type-specific expression of murine interleukin-1 receptor type I. *J. Biol. Chem.* 284:8703–8713. https://doi.org/10.1074/jbc.M808261200

Chen, V.L., N.K. Surana, J. Duan, and D.L. Kasper. 2013. Role of murine intestinal interleukin-1 receptor 1-expressing lymphoid tissue inducer-like cells in Salmonella infection. *PLoS One*. 8:e65405. https://doi.org/10.1371/journal.pone.0065405

Cheng, H.Y., M.X. Ning, D.K. Chen, and W.T. Ma. 2019. Interactions between the gut microbiota and the host innate immune response against pathogens. *Front. Immunol.* 10:607. https://doi.org/10.3389/fimmu.2019.00607

Clark, J.A., and C.M. Coopersmith. 2007. Intestinal crosstalk: A new paradigm for understanding the gut as the "motor" of critical illness. *Shock*. 28: 384–393. https://doi.org/10.1097/shk.0b013e31805569df

Coccia, M., O.J. Harrison, C. Schiering, M.J. Asquith, B. Becher, F. Powrie, and K.J. Maloy. 2012. IL-1β mediates chronic intestinal inflammation by promoting the accumulation of IL-17A secreting innate lymphoid cells and CD4(+) Th17 cells. *J. Exp. Med.* 209:1595–1609. https://doi.org/10.1084/jem.20111453

Collins, J.W., K.M. Keeney, V.F. Crepin, V.A. Rathinam, K.A. Fitzgerald, B.B. Finlay, and G. Frankel. 2014. Citrobacter rodentium: Infection, inflammation and the microbiota. *Nat. Rev. Microbiol.* 12:612–623. https://doi.org/10.1038/nrmicro3315

Cox, C.B., E.E. Storm, V.N. Kapoor, J. Chavarria-Smith, D.L. Lin, L. Wang, Y. Li, N. Kljavin, N. Ota, T.W. Bainbridge, et al. 2021. IL-1R1-dependent signaling coordinates epithelial regeneration in response to intestinal damage. *Sci. Immunol.* 6:6. https://doi.org/10.1126/sciimmunol.abe8856

Das, G., M.M. Augustine, J. Das, K. Bottomly, P. Ray, and A. Ray. 2003. An important regulatory role for CD4+CD8 alpha alpha T cells in the intestinal epithelial layer in the prevention of inflammatory bowel disease. *Proc. Natl. Acad. Sci. USA*. 100:5324–5329. https://doi.org/10.1073/pnas.0831037100

Deason, K., T.D. Troutman, A. Jain, D.K. Challa, R. Mandraju, T. Brewer, E.S. Ward, and C. Pasare. 2018. BCAP links IL-1R to the PI3K-mTOR pathway and regulates pathogenic Th17 cell differentiation. *J. Exp. Med.* 215: 2413–2428. https://doi.org/10.1084/jem.20171810

Deguine, J., and G.M. Barton. 2014. MyD88: A central player in innate immune signaling. *F1000Prime Rep.* 6:97. https://doi.org/10.12703/P6-97

Di Paolo, N.C., and D.M. Shayakhmetov. 2016. Interleukin 1α and the inflammatory process. *Nat. Immunol.* 17:906–913. https://doi.org/10.1038/ni.3503

Dmitrieva-Posocco, O., A. Dzutsev, D.F. Posocco, V. Hou, W. Yuan, V. Thovarai, I.A. Mufazalov, M. Gunzer, I.P. Shilovskiy, M.R. Khaitov, et al. 2019. Cell-type-specific responses to interleukin-1 control microbial invasion and tumor-elicited inflammation in colorectal cancer. *Immunity*. 50:166–180.e7. https://doi.org/10.1016/j.immuni.2018.11.015

Doisne, J.M., V. Soulard, C. Bécourt, L. Amniai, P. Henrot, C. Havenar-Daughton, C. Blanchet, L. Zitvogel, B. Ryffel, J.M. Cavaillon, et al. 2011. Cutting edge: Crucial role of IL-1 and IL-23 in the innate IL-17 response of peripheral lymph node NK1.1- invariant NKT cells to bacteria. *J. Immunol.* 186:662–666. https://doi.org/10.4049/jimmunol.1002725

Dryden, M. 2018. Reactive oxygen species: A novel antimicrobial. *Int. J. Antimicrob. Agents.* 51:299–303. https://doi.org/10.1016/j.ijantimicag.2017.08.029

Eichele, D.D., and K.K. Kharbanda. 2017. Dextran sodium sulfate colitis murine model: An indispensable tool for advancing our understanding of inflammatory bowel diseases pathogenesis. *World J. Gastroenterol.* 23: 6016–6029. https://doi.org/10.3748/wjg.v23.i33.6016

Frantz, A.L., E.W. Rogier, C.R. Weber, L. Shen, D.A. Cohen, L.A. Fenton, M.E. Bruno, and C.S. Kaetzel. 2012. Targeted deletion of MyD88 in intestinal epithelial cells results in compromised antibacterial immunity associated with downregulation of polymeric immunoglobulin receptor, mucin-2, and antibacterial peptides. *Mucosal Immunol.* 5:501–512. https://doi.org/10.1038/mi.2012.23

Gaffen, S.L., R. Jain, A.V. Garg, and D.J. Cua. 2014. The IL-23-IL-17 immune axis: From mechanisms to therapeutic testing. *Nat. Rev. Immunol.* 14: 585–600. https://doi.org/10.1038/nri3707

Gasse, P., C. Mary, I. Guenon, N. Noulin, S. Charron, S. Schnyder-Candrian, B. Schnyder, S. Akira, V.F. Quesniaux, V. Lagente, et al. 2007. IL-1R1/MyD88 signaling and the inflammasome are essential in pulmonary inflammation and fibrosis in mice. *J. Clin. Invest.* 117:3786–3799. https://doi.org/10.1172/JCI32285

Gibson, D.L., C. Ma, K.S. Bergstrom, J.T. Huang, C. Man, and B.A. Vallance. 2008. MyD88 signalling plays a critical role in host defence by controlling pathogen burden and promoting epithelial cell homeostasis during Citrobacter rodentium-induced colitis. *Cell. Microbiol.* 10: 618–631. https://doi.org/10.1111/j.1462-5822.2007.01071.x

Golebski, K., X.R. Ros, M. Nagasawa, S. van Tol, B.A. Heesters, H. Aglmous, C.M.A. Kradolfer, M.M. Shikhagaie, S. Seys, P.W. Hellings, et al. 2019. IL-1β, IL-23, and TGF-β drive plasticity of human ILC2s towards IL-17-producing ILCs in nasal inflammation. *Nat. Commun.* 10:2162. https://doi.org/10.1038/s41467-019-09883-7

González-Navajas, J.M., J. Law, K.P. Nguyen, M. Bhargava, M.P. Corr, N. Varki, L. Eckmann, H.M. Hoffman, J. Lee, and E. Raz. 2010. Interleukin 1 receptor signaling regulates DUBA expression and facilitates Toll-like receptor 9-driven antiinflammatory cytokine production. *J. Exp. Med.* 207:2799–2807. https://doi.org/10.1084/jem.20101326

Hausmann, A., B. Felmy, L. Kunz, S. Kroon, D.L. Berthold, G. Ganz, I. Sandu, T. Nakamura, N.S. Zangger, Y. Zhang, et al. 2021. Intercrypt sentinel macrophages tune antibacterial NF-κB responses in gut epithelial cells via TNF. *J. Exp. Med.* 218:218. https://doi.org/10.1084/jem.20210862

Hayes, P., S. Dhillon, K. O'Neill, C. Thoeni, K.Y. Hui, A. Elkadri, C.H. Guo, L. Kovacic, G. Aviello, L.A. Alvarez, et al. 2015. Defects in NADPH oxidase genes NOX1 and DUOX2 in very early onset inflammatory bowel disease. *Cell. Mol. Gastroenterol. Hepatol.* 1:489–502. https://doi.org/10.1016/j.jcmgh.2015.06.005

Hoytema van Konijnenburg, D.P., B.S. Reis, V.A. Pedicord, J. Farache, G.D. Victora, and D. Mucida. 2017. Intestinal epithelial and intraepithelial T cell crosstalk mediates a dynamic response to infection. *Cell.* 171: 783–794.e13. https://doi.org/10.1016/j.cell.2017.08.046

Hügle, B., F. Speth, and J.P. Haas. 2017. Inflammatory bowel disease following anti-interleukin-1-treatment in systemic juvenile idiopathic arthritis. *Pediatr. Rheumatol. Online J.* 15:16. https://doi.org/10.1186/s12969-017-0147-3

Irizarry-Caro, R.A., M.M. McDaniel, G.R. Overcast, V.G. Jain, T.D. Troutman, and C. Pasare. 2020. TLR signaling adapter BCAP regulates inflammatory to reparatory macrophage transition by promoting histone lactylation. *Proc. Natl. Acad. Sci. USA.* 117:30628–30638. https://doi.org/10.1073/pnas.2009778117

Ismail, A.S., K.M. Severson, S. Vaishnava, C.L. Behrendt, X. Yu, J.L. Benjamin, K.A. Ruhn, B. Hou, A.L. DeFranco, F. Yarovinsky, and L.V. Hooper. 2011. Gammadelta intraepithelial lymphocytes are essential mediators of host-microbial homeostasis at the intestinal mucosal surface. *Proc. Natl. Acad. Sci. USA.* 108:8743–8748. https://doi.org/10.1073/pnas.1019574108

Ivanov, I.I., K. Atarashi, N. Manel, E.L. Brodie, T. Shima, U. Karaoz, D. Wei, K.C. Goldfarb, C.A. Santee, S.V. Lynch, et al. 2009. Induction of intestinal Th17 cells by segmented filamentous bacteria. *Cell.* 139:485–498. https://doi.org/10.1016/j.cell.2009.09.033

Jain, A., R. Song, E.K. Wakeland, and C. Pasare. 2018. T cell-intrinsic IL-1R signaling licenses effector cytokine production by memory CD4 T cells. *Nat. Commun.* 9:3185. https://doi.org/10.1038/s41467-018-05489-7

Joshi, N.A. and J.N. Fass. 2011. Sickle: A sliding-window, adaptive, quality-based trimming tool for FastQ files. (Version 1.33) [Software].

Jung, Y., T. Wen, M.K. Mingler, J.M. Caldwell, Y.H. Wang, D.D. Chaplin, E.H. Lee, M.H. Jang, S.Y. Woo, J.Y. Seoh, et al. 2015. IL-1β in eosinophil-mediated small intestinal homeostasis and IgA production. *Mucosal Immunol.* 8:930–942. https://doi.org/10.1038/mi.2014.123

Kamada, N., K. Sakamoto, S.U. Seo, M.Y. Zeng, Y.G. Kim, M. Cascalho, B.A. Vallance, J.L. Puente, and G. Núñez. 2015. Humoral immunity in the gut selectively targets phenotypically virulent attaching-and-effacing bacteria for intraluminal elimination. *Cell Host Microbe.* 17:617–627. https://doi.org/10.1016/j.chom.2015.04.001

Kaminsky, L.W., R. Al-Sadi, and T.Y. Ma. 2021. IL-1β and the intestinal epithelial tight junction barrier. *Front. Immunol.* 12:767456. https://doi.org/10.3389/fimmu.2021.767456

Keir, M., Y. Yi, T. Lu, and N. Ghilardi. 2020. The role of IL-22 in intestinal health and disease. *J. Exp. Med.* 217:e20192195. https://doi.org/10.1084/jem.20192195

Klose, C.S., and D. Artis. 2016. Innate lymphoid cells as regulators of immunity, inflammation and tissue homeostasis. *Nat. Immunol.* 17: 765–774. https://doi.org/10.1038/ni.3489

Kobayashi, K.S., M. Chamaillard, Y. Ogura, O. Henegariu, N. Inohara, G. Nuñez, and R.A. Flavell. 2005. Nod2-dependent regulation of innate and adaptive immunity in the intestinal tract. *Science.* 307:731–734. https://doi.org/10.1126/science.1104911

Krieglstein, C.F., C. Anthoni, W.H. Cerwinka, K.Y. Stokes, J. Russell, M.B. Grisham, and D.N. Granger. 2007. Role of blood- and tissue-associated inducible nitric-oxide synthase in colonic inflammation. *Am. J. Pathol.* 170:490–496. https://doi.org/10.2353/ajpath.2007.060594

Krysko, O., T. Maes, M. Plantinga, G. Holtappels, R. Imiru, P. Vandenabeele, G. Joos, D.V. Krysko, and C. Bachert. 2013. The adjuvant-like activity of staphylococcal enterotoxin B in a murine asthma model is independent of IL-1R signaling. *Allergy.* 68:446–453. https://doi.org/10.1111/all.12102

Lebeis, S.L., K.R. Powell, D. Merlin, M.A. Sherman, and D. Kalman. 2009. Interleukin-1 receptor signaling protects mice from lethal intestinal damage caused by the attaching and effacing pathogen Citrobacter rodentium. *Infect. Immun.* 77:604–614. https://doi.org/10.1128/IAI.00907-08

Lei-Leston, A.C., A.G. Murphy, and K.J. Maloy. 2017. Epithelial cell inflammasomes in intestinal immunity and inflammation. *Front. Immunol.* 8:1168. https://doi.org/10.3389/fimmu.2017.01168

Leoni, G., P.A. Neumann, R. Sumagin, T.L. Denning, and A. Nusrat. 2015. Wound repair: Role of immune-epithelial interactions. *Mucosal Immunol.* 8:959–968. https://doi.org/10.1038/mi.2015.63

Liang, S.C., X.Y. Tan, D.P. Luxenberg, R. Karim, K. Dunussi-Joannopoulos, M. Collins, and L.A. Fouser. 2006. Interleukin (IL)-22 and IL-17 are coexpressed by Th17 cells and cooperatively enhance expression of antimicrobial peptides. *J. Exp. Med.* 203:2271–2279. https://doi.org/10.1084/jem.20061308

Lipinski, S., A. Till, C. Sina, A. Arlt, H. Grasberger, S. Schreiber, and P. Rosenstiel. 2009. DUOX2-derived reactive oxygen species are effectors of NOD2-mediated antibacterial responses. *J. Cell Sci.* 122:3522–3530. https://doi.org/10.1242/jcs.050690

Lopez-Castejon, G., and D. Brough. 2011. Understanding the mechanism of IL-1β secretion. *Cytokine Growth Factor Rev.* 22:189–195. https://doi.org/10.1016/j.cytogfr.2011.10.001

Love, M.I., W. Huber, and S. Anders. 2014. Moderated estimation of fold change and dispersion for RNA-seq data with DESeq2. *Genome Biol.* 15: 550. https://doi.org/10.1186/s13059-014-0550-8

MacFie, T.S., R. Poulsom, A. Parker, G. Warnes, T. Boitsova, A. Nijhuis, N. Suraweera, A. Poehlmann, J. Szary, R. Feakins, et al. 2014. DUOX2 and DUOXA2 form the predominant enzyme system capable of producing the reactive oxygen species H2O2 in active ulcerative colitis and are modulated by 5-aminosalicylic acid. *Inflamm. Bowel Dis.* 20:514–524. https://doi.org/10.1097/01.MIB.0000442012.45038.0e

Macpherson, A.J., and T. Uhr. 2004. Compartmentalization of the mucosal immune responses to commensal intestinal bacteria. *Ann. N. Y. Acad. Sci.* 1029:36–43. https://doi.org/10.1196/annals.1309.005

Mao, L., A. Kitani, W. Strober, and I.J. Fuss. 2018. The role of NLRP3 and IL-1β in the pathogenesis of inflammatory bowel disease. *Front. Immunol.* 9:2566. https://doi.org/10.3389/fimmu.2018.02566

Marr, K.A., S.A. Balajee, T.R. Hawn, A. Ozinsky, U. Pham, S. Akira, A. Aderem, and W.C. Liles. 2003. Differential role of MyD88 in macrophage-mediated responses to opportunistic fungal pathogens. *Infect. Immun.* 71:5280–5286. https://doi.org/10.1128/IAI.71.9.5280-5286.2003

McEntee, C.P., C.M. Finlay, and E.C. Lavelle. 2019. Divergent roles for the IL-1 family in gastrointestinal homeostasis and inflammation. *Front. Immunol.* 10:1266. https://doi.org/10.3389/fimmu.2019.01266

McGee, D.W., S.J. Vitkus, and P. Lee. 1996. The effect of cytokine stimulation on IL-1 receptor mRNA expression by intestinal epithelial cells. *Cell. Immunol.* 168:276–280. https://doi.org/10.1006/cimm.1996.0076

McKenzie, S.J., M.S. Baker, G.D. Buffinton, and W.F. Doe. 1996. Evidence of oxidant-induced injury to epithelial cells during inflammatory bowel disease. *J. Clin. Invest.* 98:136–141. https://doi.org/10.1172/JCI118757

Menendez, A., B.P. Willing, M. Montero, M. Wlodarska, C.C. So, G. Bhinder, B.A. Vallance, and B.B. Finlay. 2013. Bacterial stimulation of the TLR-MyD88 pathway modulates the homeostatic expression of ileal Paneth cell α-defensins. *J. Innate Immun.* 5:39–49. https://doi.org/10.1159/000341630

Menghini, P., D. Corridoni, L.F. Buttó, A. Osme, S. Shivaswamy, M. Lam, G. Bamias, T.T. Pizarro, A. Rodriguez-Palacios, C.A. Dinarello, and F. Cominelli. 2019. Neutralization of IL-1α ameliorates Crohn's disease-like ileitis by functional alterations of the gut microbiome. *Proc. Natl. Acad. Sci. USA.* 116:26717–26726. https://doi.org/10.1073/pnas.1915043116

Miyoshi, H., K.L. VanDussen, N.P. Malvin, S.H. Ryu, Y. Wang, N.M. Sonnek, C.W. Lai, and T.S. Stappenbeck. 2017. Prostaglandin E2 promotes intestinal repair through an adaptive cellular response of the epithelium. *EMBO J.* 36:5–24. https://doi.org/10.15252/embj.201694660

Moon, C., K.L. VanDussen, H. Miyoshi, and T.S. Stappenbeck. 2014. Development of a primary mouse intestinal epithelial cell monolayer culture system to evaluate factors that modulate IgA transcytosis. *Mucosal Immunol.* 7:818–828. https://doi.org/10.1038/mi.2013.98

Mowat, A.M., and W.W. Agace. 2014. Regional specialization within the intestinal immune system. *Nat. Rev. Immunol.* 14:667–685. https://doi.org/10.1038/nri3738

Mullineaux-Sanders, C., J. Sanchez-Garrido, E.G.D. Hopkins, A.R. Shenoy, R. Barry, and G. Frankel. 2019. Citrobacter rodentium-host-microbiota interactions: Immunity, bioenergetics and metabolism. *Nat. Rev. Microbiol.* 17:701–715. https://doi.org/10.1038/s41579-019-0252-z

Muzaki, A.R., P. Tetlak, J. Sheng, S.C. Loh, Y.A. Setiagani, M. Poidinger, F. Zolezzi, K. Karjalainen, and C. Ruedl. 2016. Intestinal CD103(+)CD11b(-) dendritic cells restrain colitis via IFN-γ-induced anti-inflammatory response in epithelial cells. *Mucosal Immunol.* 9:336–351. https://doi.org/10.1038/mi.2015.64

Natividad, J.M., V. Petit, X. Huang, G. de Palma, J. Jury, Y. Sanz, D. Philpott, C.L. Garcia Rodenas, K.D. McCoy, and E.F. Verdu. 2012. Commensal and probiotic bacteria influence intestinal barrier function and susceptibility to colitis in Nod1$^{-/-}$; Nod2$^{-/-}$ mice. *Inflamm. Bowel Dis.* 18:1434–1446. https://doi.org/10.1002/ibd.22848

Nowarski, R., R. Jackson, N. Gagliani, M.R. de Zoete, N.W. Palm, W. Bailis, J.S. Low, C.C. Harman, M. Graham, E. Elinav, and R.A. Flavell. 2015. Epithelial IL-18 equilibrium controls barrier function in colitis. *Cell.* 163:1444–1456. https://doi.org/10.1016/j.cell.2015.10.072

Okada, T., S. Fukuda, K. Hase, S. Nishiumi, Y. Izumi, M. Yoshida, T. Hagiwara, R. Kawashima, M. Yamazaki, T. Oshio, et al. 2013. Microbiota-derived lactate accelerates colon epithelial cell turnover in starvation-refed mice. *Nat. Commun.* 4:1654. https://doi.org/10.1038/ncomms2668

Oksanen, J., G.F. Blanchet, R. Kindt, P. Legendre, P.R. Minchin, R.B. O'Hara, G.L. Simpson, P.M. Solymos, H.H. Stevens, and H. Wagner. 2015. vegan: Community ecology package. http://CRAN.R-project.org/package=vegan.

Okumura, R., and K. Takeda. 2018. Maintenance of intestinal homeostasis by mucosal barriers. *Inflamm. Regen.* 38:5. https://doi.org/10.1186/s41232-018-0063-z

Parks, O.B., D.A. Pociask, Z. Hodzic, J.K. Kolls, and M. Good. 2016. Interleukin-22 signaling in the regulation of intestinal health and disease. *Front. Cell Dev. Biol.* 3:85. https://doi.org/10.3389/fcell.2015.00085

Peterson, L.W., and D. Artis. 2014. Intestinal epithelial cells: Regulators of barrier function and immune homeostasis. *Nat. Rev. Immunol.* 14:141–153. https://doi.org/10.1038/nri3608

Pickert, G., C. Neufert, M. Leppkes, Y. Zheng, N. Wittkopf, M. Warntjen, H.A. Lehr, S. Hirth, B. Weigmann, S. Wirtz, et al. 2009. STAT3 links IL-22 signaling in intestinal epithelial cells to mucosal wound healing. *J. Exp. Med.* 206:1465–1472. https://doi.org/10.1084/jem.20082683

Price, A.E., K. Shamardani, K.A. Lugo, J. Deguine, A.W. Roberts, B.L. Lee, and G.M. Barton. 2018. A map of toll-like receptor expression in the intestinal epithelium reveals distinct spatial, cell type-specific, and temporal patterns. *Immunity.* 49:560–575.e6. https://doi.org/10.1016/j.immuni.2018.07.016

Rakoff-Nahoum, S., J. Paglino, F. Eslami-Varzaneh, S. Edberg, and R. Medzhitov. 2004. Recognition of commensal microflora by toll-like receptors is required for intestinal homeostasis. *Cell.* 118:229–241. https://doi.org/10.1016/j.cell.2004.07.002

Rauch, I., K.A. Deets, D.X. Ji, J. von Moltke, J.L. Tenthorey, A.Y. Lee, N.H. Philip, J.S. Ayres, I.E. Brodsky, K. Gronert, and R.E. Vance. 2017. NAIP-NLRC4 inflammasomes coordinate intestinal epithelial cell expulsion with eicosanoid and IL-18 release via activation of caspase-1 and -8. *Immunity.* 46:649–659. https://doi.org/10.1016/j.immuni.2017.03.016

Rhen, M. 2019. Salmonella and reactive oxygen species: A love-hate relationship. *J. Innate Immun.* 11:216–226. https://doi.org/10.1159/000496370

Robson, M.J., C.B. Zhu, M.A. Quinlan, D.A. Botschner, N.L. Baganz, K.M. Lindler, J.G. Thome, W.A. Hewlett, and R.D. Blakely. 2016. Generation and characterization of mice expressing a conditional allele of the interleukin-1 receptor type 1. *PLoS One.* 11:e0150068. https://doi.org/10.1371/journal.pone.0150068

Rodríguez-Colman, M.J., M. Schewe, M. Meerlo, E. Stigter, J. Gerrits, M. Pras-Raves, A. Sacchetti, M. Hornsveld, K.C. Oost, H.J. Snippert, et al. 2017. Interplay between metabolic identities in the intestinal crypt supports stem cell function. *Nature.* 543:424–427. https://doi.org/10.1038/nature21673

Seo, S.U., N. Kamada, R. Muñoz-Planillo, Y.G. Kim, D. Kim, Y. Koizumi, M. Hasegawa, S.D. Himpsl, H.P. Browne, T.D. Lawley, et al. 2015. Distinct commensals induce interleukin-1β via NLRP3 inflammasome in inflammatory monocytes to promote intestinal inflammation in response to injury. *Immunity.* 42:744–755. https://doi.org/10.1016/j.immuni.2015.03.004

Silberger, D.J., C.L. Zindl, and C.T. Weaver. 2017. Citrobacter rodentium: A model enteropathogen for understanding the interplay of innate and adaptive components of type 3 immunity. *Mucosal Immunol.* 10:1108–1117. https://doi.org/10.1038/mi.2017.47

Song, A., L. Zhu, G. Gorantla, O. Berdysz, S.A. Amici, M. Guerau-de-Arellano, K.M. Madalena, J.K. Lerch, X. Liu, and N. Quan. 2018a. Salient type 1 interleukin 1 receptor expression in peripheral non-immune cells. *Sci. Rep.* 8:723. https://doi.org/10.1038/s41598-018-19248-7

Song, J., Z. Chen, T. Geng, M. Wang, S. Yi, K. Liu, W. Zhou, J. Gao, W. Song, and H. Tang. 2018b. Deleting MyD88 signaling in myeloid cells promotes development of adenocarcinomas of the colon. *Cancer Lett.* 433:65–75. https://doi.org/10.1016/j.canlet.2018.06.036

Spehlmann, M.E., S.M. Dann, P. Hruz, E. Hanson, D.F. McCole, and L. Eckmann. 2009. CXCR2-dependent mucosal neutrophil influx protects against colitis-associated diarrhea caused by an attaching/effacing lesion-forming bacterial pathogen. *J. Immunol.* 183:3332–3343. https://doi.org/10.4049/jimmunol.0900600

Staerck, C., A. Gastebois, P. Vandeputte, A. Calenda, G. Larcher, L. Gillmann, N. Papon, J.P. Bouchara, and M.J.J. Fleury. 2017. Microbial antioxidant defense enzymes. *Microb. Pathog.* 110:56–65. https://doi.org/10.1016/j.micpath.2017.06.015

Sutherland, D.B., G.W. Varilek, and G.A. Neil. 1994. Identification and characterization of the rat intestinal epithelial cell (IEC-18) interleukin-1 receptor. *Am. J. Physiol.* 266:C1198–C1203. https://doi.org/10.1152/ajpcell.1994.266.5.C1198

Sutton, C.E., S.J. Lalor, C.M. Sweeney, C.F. Brereton, E.C. Lavelle, and K.H. Mills. 2009. Interleukin-1 and IL-23 induce innate IL-17 production from gammadelta T cells, amplifying Th17 responses and autoimmunity. *Immunity.* 31:331–341. https://doi.org/10.1016/j.immuni.2009.08.001

Vaishnava, S., C.L. Behrendt, A.S. Ismail, L. Eckmann, and L.V. Hooper. 2008. Paneth cells directly sense gut commensals and maintain homeostasis at the intestinal host-microbial interface. *Proc. Natl. Acad. Sci. USA.* 105:20858–20863. https://doi.org/10.1073/pnas.0808723105

VanDussen, K.L., J.M. Marinshaw, N. Shaikh, H. Miyoshi, C. Moon, P.I. Tarr, M.A. Ciorba, and T.S. Stappenbeck. 2015. Development of an enhanced human gastrointestinal epithelial culture system to facilitate patient-based assays. *Gut.* 64:911–920. https://doi.org/10.1136/gutjnl-2013-306651

VanDussen, K.L., N.M. Sonnek, and T.S. Stappenbeck. 2019. L-WRN conditioned medium for gastrointestinal epithelial stem cell culture shows replicable batch-to-batch activity levels across multiple research teams. *Stem Cell Res.* 37:101430. https://doi.org/10.1016/j.scr.2019.101430

Villeret, B., L. Brault, A. Couturier-Maillard, P. Robinet, V. Vasseur, T. Secher, I. Dimier-Poisson, M. Jacobs, S.G. Zheng, V.F. Quesniaux, and B. Ryffel. 2013. Blockade of IL-1R signaling diminishes Paneth cell depletion and Toxoplasma gondii induced ileitis in mice. *Am. J. Clin. Exp. Immunol.* 2:107–116

Wahida, A., M. Müller, A. Hiergeist, B. Popper, K. Steiger, C. Branca, M. Tschurtschenthaler, T. Engleitner, S. Donakonda, J. De Coninck, et al. 2021. XIAP restrains TNF-driven intestinal inflammation and dysbiosis by promoting innate immune responses of Paneth and dendritic cells. *Sci. Immunol.* 6:eabf7235. https://doi.org/10.1126/sciimmunol.abf7235

Wéra, O., P. Lancellotti, and C. Oury. 2016. The dual role of neutrophils in inflammatory bowel diseases. *J. Clin. Med.* 5:5. https://doi.org/10.3390/jcm5120118

Whitley, S.K., A. Balasubramani, C.L. Zindl, R. Sen, Y. Shibata, G.E. Crawford, N.M. Weathington, R.D. Hatton, and C.T. Weaver. 2018. IL-1R signaling promotes STAT3 and NF-κB factor recruitment to distal cis-regulatory elements that regulate Il17a/f transcription. *J. Biol. Chem.* 293:15790–15800. https://doi.org/10.1074/jbc.RA118.002721

Wickham, H. 2016. ggplot2: Elegant Graphics for Data Analysis. Springer-Verlag, New York.

Wood, D.E., and S.L. Salzberg. 2014. Kraken: Ultrafast metagenomic sequence classification using exact alignments. *Genome Biol.* 15:R46. https://doi.org/10.1186/gb-2014-15-3-r46

Wrzosek, L., S. Miquel, M.L. Noordine, S. Bouet, M. Joncquel Chevalier-Curt, V. Robert, C. Philippe, C. Bridonneau, C. Cherbuy, C. Robbe-Masselot, et al. 2013. Bacteroides thetaiotaomicron and Faecalibacterium prausnitzii influence the production of mucus glycans and the development of goblet cells in the colonic epithelium of a gnotobiotic model rodent. *BMC Biol.* 11:61. https://doi.org/10.1186/1741-7007-11-61

Xia, Y., and J. Sun. 2017. Hypothesis testing and statistical analysis of microbiome. *Genes Dis.* 4:138–148. https://doi.org/10.1016/j.gendis.2017.06.001

Yoshida, H., J. Russell, E.Y. Senchenkova, L.D. Almeida Paula, and D.N. Granger. 2010. Interleukin-1beta mediates the extra-intestinal thrombosis associated with experimental colitis. *Am. J. Pathol.* 177:2774–2781. https://doi.org/10.2353/ajpath.2010.100205

Zhao, M., S. Tang, J. Xin, Y. Wei, and D. Liu. 2018. Reactive oxygen species induce injury of the intestinal epithelium during hyperoxia. *Int. J. Mol. Med.* 41:322–330. https://doi.org/10.3892/ijmm.2017.3247

Zheng, Y., P.A. Valdez, D.M. Danilenko, Y. Hu, S.M. Sa, Q. Gong, A.R. Abbas, Z. Modrusan, N. Ghilardi, F.J. de Sauvage, and W. Ouyang. 2008. Interleukin-22 mediates early host defense against attaching and effacing bacterial pathogens. *Nat. Med.* 14:282–289. https://doi.org/10.1038/nm1720

JEM

Supplemental material

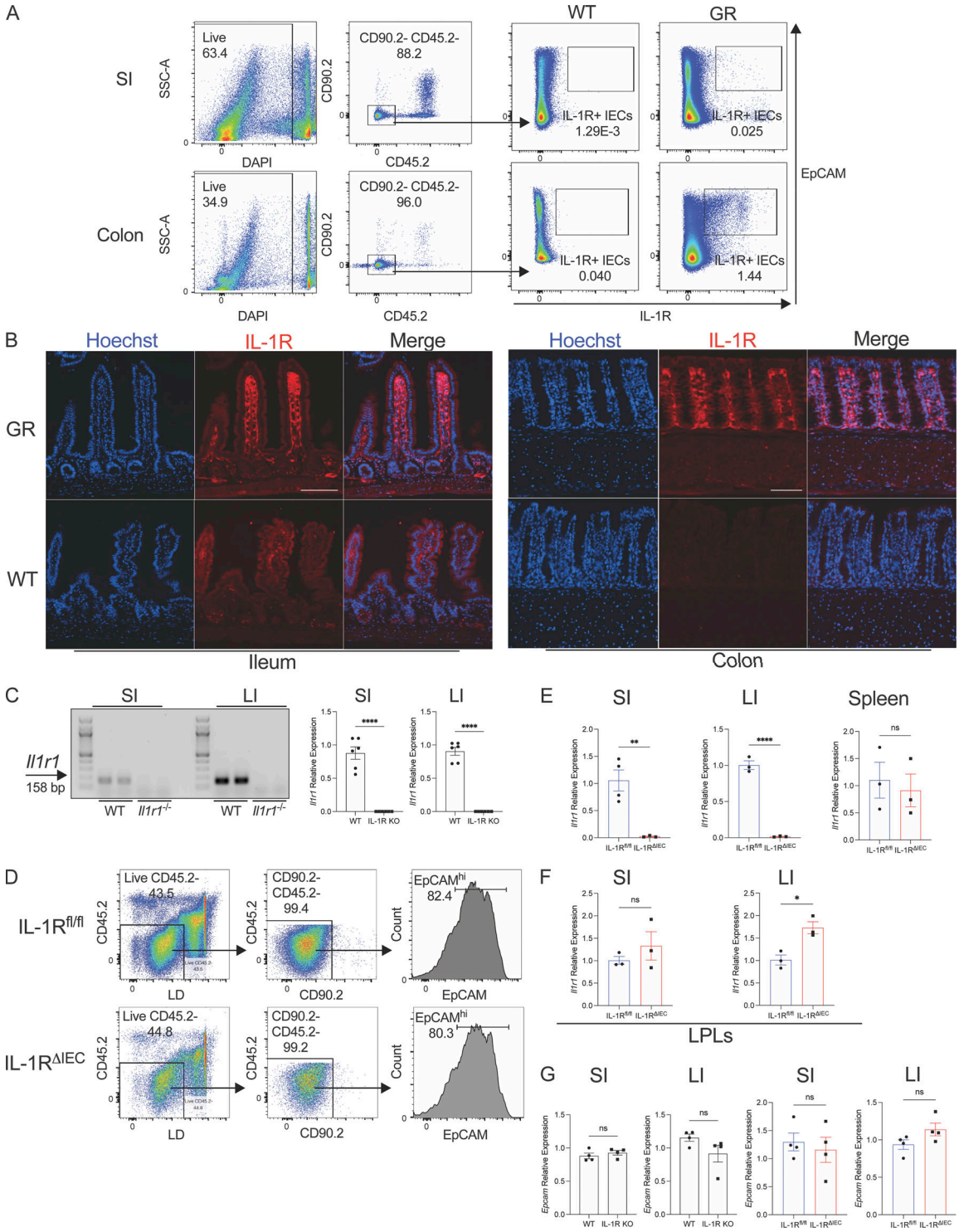

Figure S1. **Analysis of IEC expression of IL-1R. (A)** Gating strategy after enrichment of IECs from the colon and small intestine (SI) of WT mice. IECs are pregated as Live CD45.2$^-$ CD90.2$^-$ EpCAM^{hi} cells. EpCAM^{hi} IECs from WT and IL-1R$^{GR/GR}$ mice (GR) which co-express TdTomato (red) were then examined for IL-1R expression by flow cytometry. Representative flow cytometry plots gated on IECs (Live CD45.2$^-$ CD90.2$^-$) enriched from the small intestine or colon from WT and GR mice are shown. **(B)** Histological sections of the ileum and colon of WT or IL-1R$^{GR/GR}$ mice (GR) which co-express TdTomato (red) with IL-1R were counterstained with Hoechst (blue). Scale = 100 µm. **(C)** PCR and real-time qPCR amplification using *Il1r1*-specific primers on cDNA isolated from enriched IECs in the small intestine and colon of WT and *Il1r1*$^{-/-}$ (IL-1R KO) mice. **(D)** Gating strategy after enrichment of IECs in the colon of IL-1R$^{fl/fl}$ and IL-1R$^{\Delta IEC}$ mice. Live CD45.2$^-$ CD90.2$^-$ EpCAM^{hi} cells are considered to be IECs. **(E)** *Il1r1* expression was measured from IECs in the ileum (left), the colon (middle), or total splenocytes (right). **(F)** *Il1r1* expression was measured from LPLs in the ileum (left) or the colon (right). **(G)** *Epcam* expression was measured from IECs in the ileum or the colon of WT and IL-1R KO mice (left) or of IL-1R$^{fl/fl}$ and IL-1R$^{\Delta IEC}$ mice (right). Data represent two independent experiments are shown as ± SEM of biological replicates. *P < 0.05, **P < 0.01, and ****P < 0.0001. **(C and E–G)** Unpaired *t* test. LI, large intestine. Source data are available for this figure: SourceData FS1.

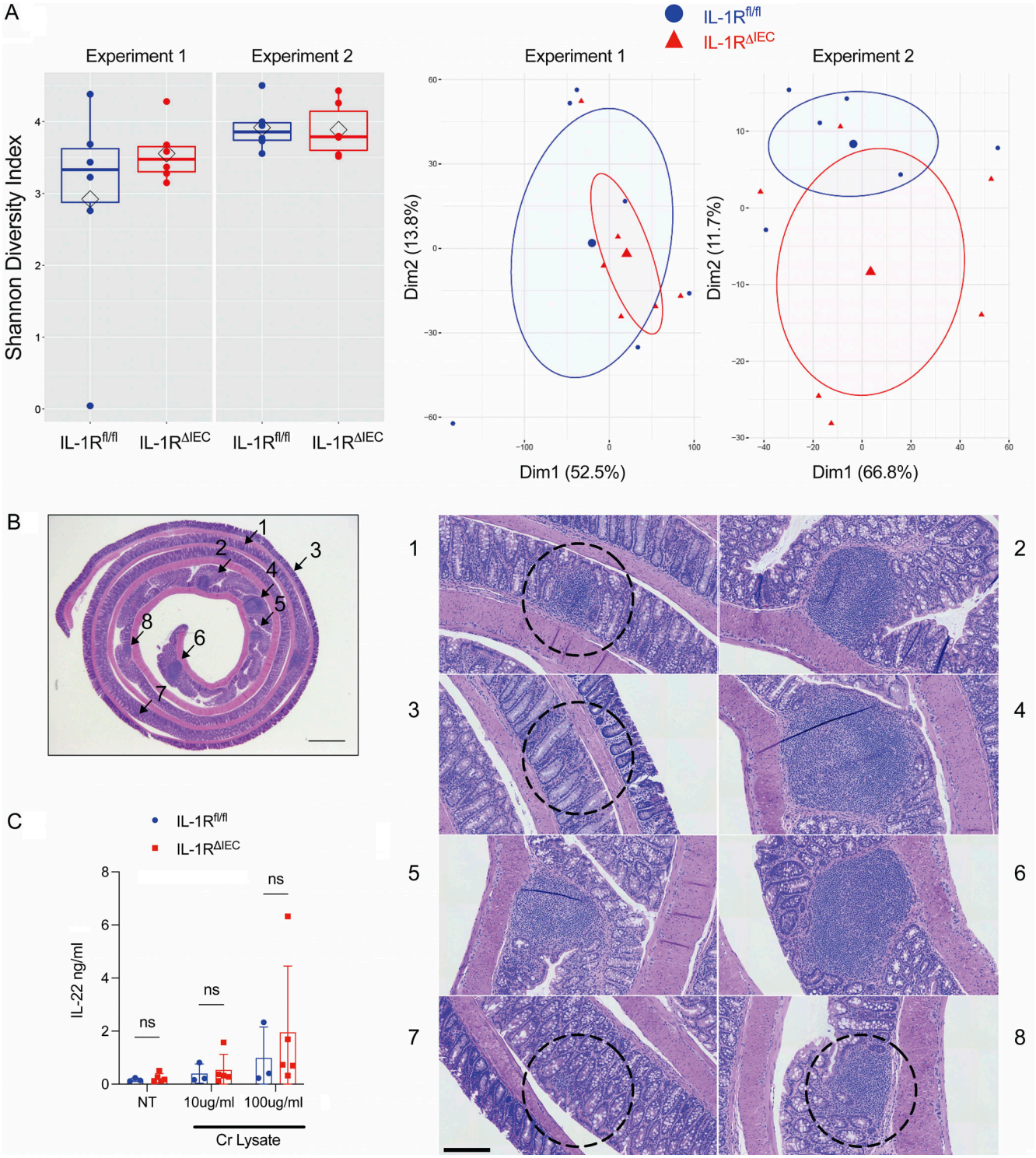

Figure S2. **Lack of IL-1R on epithelial cells does not affect commensal microbiota composition, yet *C. rodentium* induces more pathology in mice that lack IL-1R in IECs. (A)** IL-1R$^{fl/fl}$ and IL-1R$^{\Delta IEC}$ mice harbor very similar populations of commensal microbiota in their intestines. Shannon diversity index (left) and principal component analysis plots (right) of fecal microbiota collected from two independent litters of mice. **(B)** H&E-stained colon sections at day 37 after *C. rodentium* infection. Colons obtained from IL-1R$^{\Delta IEC}$ mice showing higher magnification of black arrow regions (left) which indicate areas of concentrated immune cell infiltration (right). Dotted circles are drawn on some areas to focus on specific areas of inflammatory cell infiltration. Scale = 1,000 µm (left panel) and 200 µm (right panels). **(C)** IL-22 ELISA on supernatants of mesenteric lymph node cells from *C. rodentium*–infected mice cultured in the presence of indicated concentrations of *C. rodentium* (Cr) lysate for 3 d. Data represent two independent experiments are show mean ± SEM of biological replicates. Unpaired *t* test.

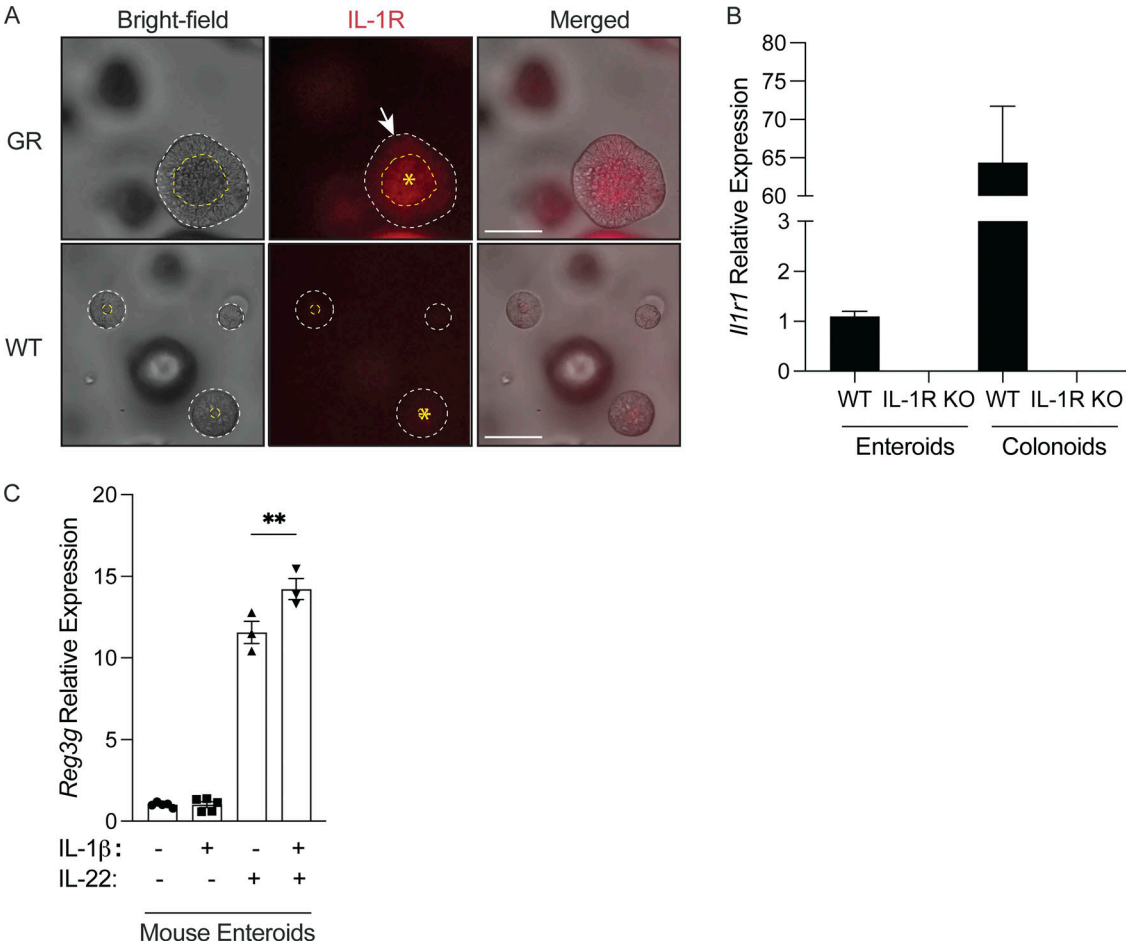

Figure S3. **IL-1β synergizes with IL-22 to drive an antimicrobial gene program in enteroids and colonoids. (A)** TdTomato fluorescence or bright-field microscopy images of live, differentiated colonoids derived from IL-1R$^{GR/GR}$ (GR) or WT control mice. Dotted lines outline the colonoids, and dead cell debris is indicated by asterisks. Scale = 100 µm. **(B)** Gene expression was quantitated by qPCR of *Il1r1* in mouse enteroids and colonoids derived from either WT or IL-1R KO mice. **(C)** *Reg3g* expression was quantitated by qPCR in enteroids derived from WT mice after a 12-h stimulation by IL-1β (100 ng/ml), IL-22 (1 ng/ml), or a combination of both. Data represent two independent experiments and show mean ± SEM of biological triplicates. **P < 0.01. **(C)** One-way ANOVA.

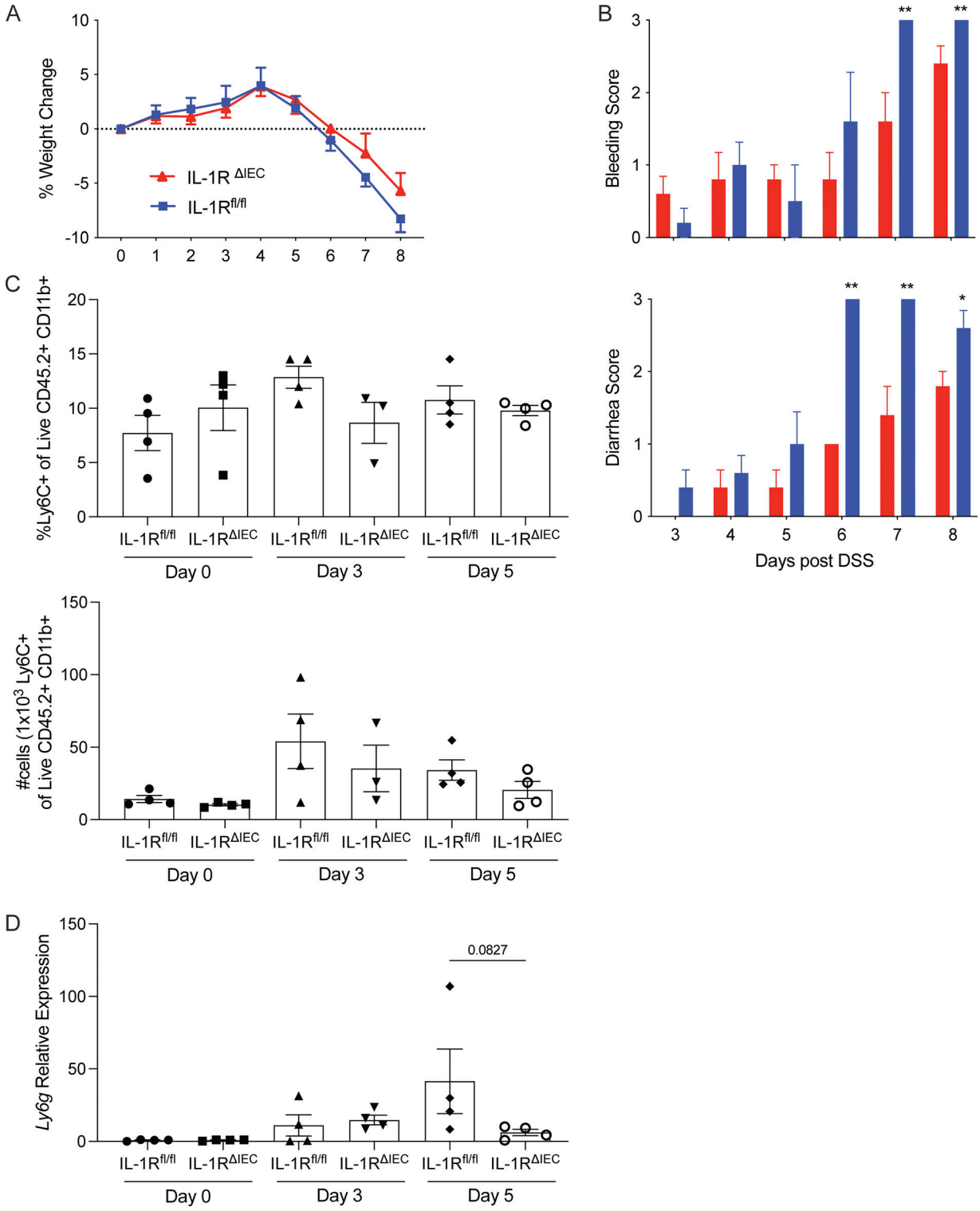

Figure S4. **Mice lacking IL-1R expression on IECs are resistant to DSS-induced colitis. (A)** Representative daily weight change of IL-1R$^{fl/fl}$ (n = 12) and IL-1R$^{\Delta IEC}$ (n = 12) mice given a 2% DSS solution in drinking water for 8 d. **(B)** Daily observations were made to determine rectal bleeding (top) and stool consistency (bottom) of the mice given DSS. **(C)** Flow cytometric analysis of cell percentages (top) and numbers (bottom) of lamina propria cells showing inflammatory monocyte infiltration (gated on Live CD45.2$^+$ CD11b$^+$ cells—inflammatory monocytes considered Ly6C$^+$ Ly6G$^-$ population) at steady state (day 0), day 3, and day 5 after administration of 2% DSS in drinking water. **(D)** *Ly6g* expression was quantitated by qPCR as a proxy for neutrophil infiltration in colon tissue of mice at steady state (day 0) or given 2% DSS in drinking water for 3 or 5 d. Data represent three independent experiments and show means ± SEM of biological replicates. *P < 0.05, **P < 0.01. **(B)** Multiple unpaired t tests. **(D)** Unpaired t test.

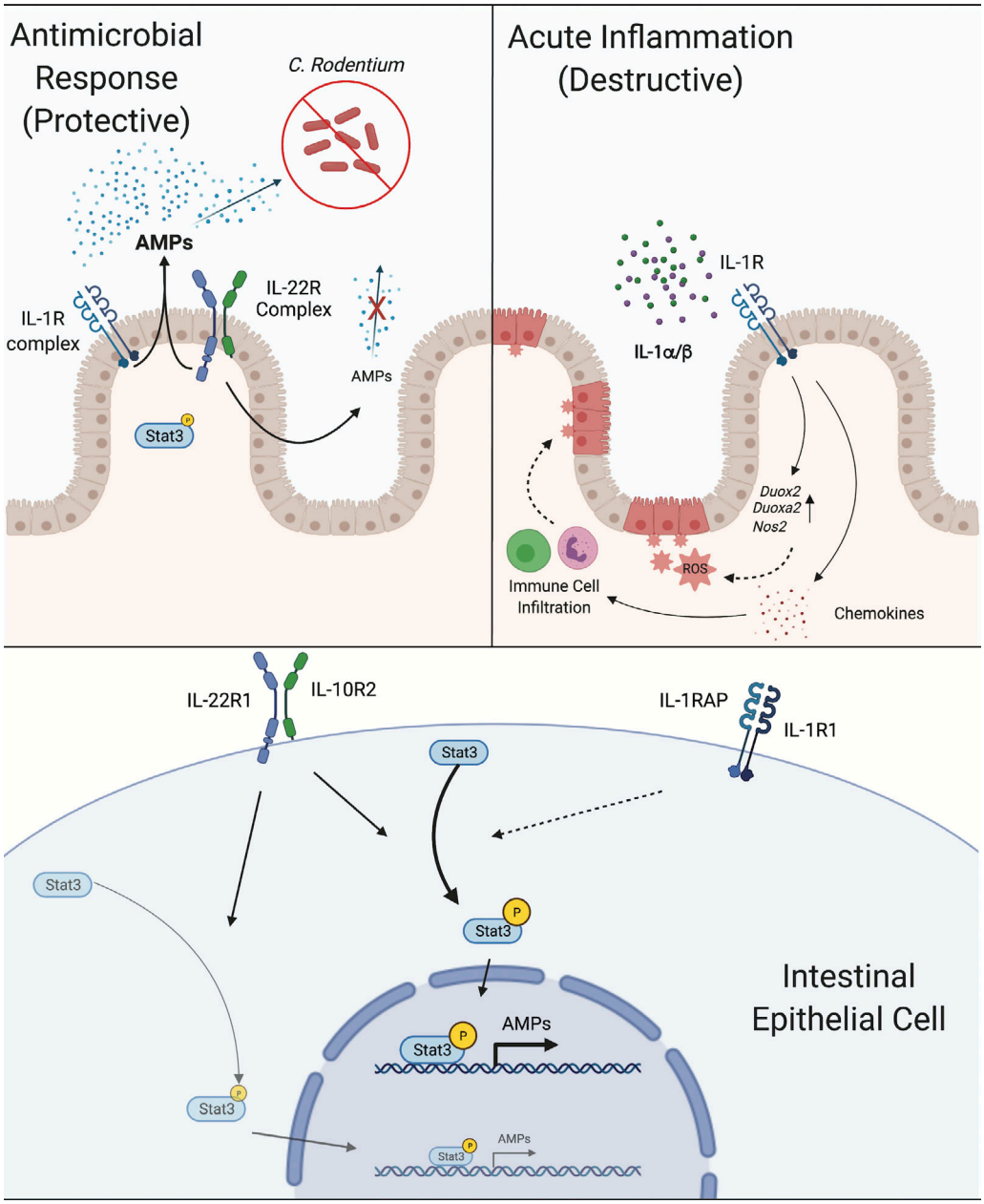

Figure S5. **Dual role for IL-1R signaling in IECs in driving antimicrobial response and pathology during colitis.** Top left: IEC-intrinsic IL-1R synergizes with IL-22R to drive optimal antimicrobial production, which protects against intestinal pathogens such as *C. rodentium*. In the absence of IL-1R there is sub-optimal AMP induction by IL-22, which results in the inability to clear intestinal pathogens. Top right: During acute inflammation, IL-1α/β lead to excessive IL-1R signaling, which results in immune cell recruitment and production of ROS/RNS that is damaging to the IEC barrier. Bottom: Simultaneous stimulation of IL-1R and IL-22R on IECs results in enhanced phosphorylation of STAT3 to drive robust production of AMPs.